Characterization of Cold-Sprayed Copper Coatings and comparison with Wrought Copper using Miniaturized Shear Punch Tests (SPT)

by

Neeraj Sanjay Karmarkar

A thesis submitted in partial fulfillment
of the requirements for the degree of
Master of Science in Engineering
(Manufacturing Systems Engineering)
in the University of Michigan-Dearborn
2018

Master's Thesis Committee:

Professor Pravansu S. Mohanty, Chair
Associate Professor Gargi Ghosh
Assistant Professor Tanjore V. Jayaraman

Acknowledgements

First and foremost, I would like to thank my parents Dr. Sanjay N Karmarkar and Mrs. Saroj S Karmarkar for their constant love and support. I thank them for always believing me. I would like to express my gratitude to my advisor Dr. Pravansu S. Mohanty for giving me this wonderful opportunity to work at Additive Manufacturing and Process Laboratory and explore the field of thermal spray especially Laser Assisted Cold spray process. He has taught me to be an independent and innovative thinker. He has always been a constant support through various ups and downs during my master's study. I would also like to express my gratitude to my committee members Dr. Gargi Ghosh & Dr. Tanjore V. Jayaraman for helping me shape and achieve this goal. I also express my gratitude towards Mr. Kent Herrick for his contribution in collaborative work with Spee3D (an Australian based manufacturing company).

I am grateful to Dr. German Reyes who gave access and allowed me to work on the Instron machines at Manufacturing Laboratory for one of my experimentation analysis. I would also like to thank Mr. Prakash Pariti for his help in training me for the Instron machine at Manufacturing Laboratory.

I would also like to thank my past and present members and team mates of Additive and Manufacturing Laboratory, my teammates: Dr. Vikram Varadaraajan, Ramcharan Palacode Visverwaran, Praneet Talwar, Sharan Nagendiaran, Aniket Jadhav who have always been there for the discussions, support and encouragement. I am also thankful to my friends Prajwal C, Narendra M, Mayuresh S, Prakash P, Abhishek M, Abhishek K, Saurabh M, Vishwajeet R and Sanket D for their support throughout the study.

Preface

The thesis highlights a study to co-relate the tensile strength and shear strength of cold-sprayed copper along with measurement of mechanicals properties like Vickers hardness and Electrical Conductivity with characterization using SEM.

Chapter 1 is an introduction to the trending concept of Additive Manufacturing. With a brief about Cold-spray technology used for this study.

Chapter 2 entails about the Aim and Scope of the thesis.

Chapter 3 is a summary of working of the cold-spray technique which is a traditional thermal spray developed by a Russian scientist Dr. Papyrin.

Chapter 4 includes all the type of experiments done for this study. It also briefs in detail about the equipment's and parameters used for the experimentation.

Chapter 5 includes the experimental results of tensile tests, shear punch tests. It also includes a possible co-relation displayed between tensile strength and shear strength. The experimental data is also supported with hardness and electrical conductivity measurements along with characterization of cold-sprayed coatings.

Table of Contents

Acknowledgements....iii

Preface....ii

List of Figures vi

List of Tables ix

Abstract x

Chapter 1 Introduction 1

1.1 Introduction to Additive Manufacturing 1

1.2 Limitation in Additive Manufacturing 2

1.3 Cold Spray Technology 2

Chapter 2 Aim and Scope for the Research 4

2.1 Aim 4

2.2 Scope 5

Chapter 3 Cold spray 6

3.1 Particle velocity and temperature 6

3.2 Nozzle Design 8

3.3 Bonding Mechanism.... 9

3.4 Standoff distance 10

Chapter 4 Characterization and Experimental 12

Characterization and Analysis....12

4.1 UTM (Universal Testing Machine) 12

4.1.1 Tensile Tests 12

4.1.2 Shear Punch Tests 13

4.2 Microstructural Characterization.... 14

4.3 Vickers Hardness 15

4.4 Electrical Conductivity 16

Chapter 5 Results and Discussion 17

5.1 Cold-Spray.... 17

5.2 Heat Treatment 19

5.3 Design of Experiments 20
5.4 Tensile Tests 20
5.4.1 Cu-11000 20
5.4.2 Copper As Spray 22
5.4.2.1 Copper-AS-Horizontal Orientation 22
5.4.2.2 Copper-AS-Edge Orientation 23
5.4.2.3 Copper-AS-Vertical Orientation 24
5.4.3 Copper 400C heat-treat 25
5.4.4 Copper 600C heat-treat 26
5.5 Shear Punch Tests 27
5.5.1 Cu-11000 28
5.5.2 Copper As Spray 29
5.5.2.1 Copper-AS-Horizontal Orientation 29
5.5.2.2 Copper-AS-Edge Orientation 30
5.5.2.3 Copper-AS-Vertical Orientation 30
5.5.3 Copper 400C heat-treat 31
5.5.4 Copper 600C heat-treat 31
5.6 Co-relation of SPT and Tensile test 32
5.7 Electrical Conductivity 34
5.8 VickersHardness 35
5.9 SEM Images 36
5.9.1 Etched Coatings 37
5.9.2 Shear Punch Cracks 39
Chapter 6 Conclusion and Future Study 41
6.1 Conclusion 41
6.2 Future Study 42
References 43

List of Figures

Figure 1 Types of AM Techniques [5] 1

Figure 2 Cold Spray Process Block Diagram [4].. 2

Figure 3 A sample Dog-bone as per ASTM E8 [9] 4

Figure 4 Representation of powder and Particle acceleration to Coating formation [4] 6

Figure 5 Effect of gas temperature on coating thickness [4] 7

Figure 6 Effect of parameters on Critical velocity and Impact particle velocity [10] 8

Figure 7 Nozzles used in cold-spray technology [4] 8

Figure 8 Schematic of Coating Deposition [4] 9

Figure 9 Stress curves for isothermal material, adiabatic material and following an adiabatic shear localization [12] 10

Figure 10 Effect of standoff distance on the calculated gas and Cu particle (40 µm) temperatures close to substrate [13] 11

Figure 11 OM images of Al coatings with standoff distances of (a) 10 mm, (b) 30 mm, (c) 50 mm [13] 11

Figure 12 Dog Bone as per ASTM E8 [8] 12

Figure 13 Experimental setup for SPT.. 14

Figure 14 HITACHI Scanning Electron Microscope 14

Figure 15 Vickers Hardness Tester.. 15

Figure 16 Eddy-current Conductivitymeter 16

Figure 17 Measurement done on a sample copper bar 16

Figure 18 Typical Cold Spray System [4] 17

Figure 19 Sprayed Copper Coatings on 6061 substrates manufactured at Spee3D L to R Horizontal, Edge, Vertical 18

Figure 20 CAD representation a) Edge b) Vertical c) Horizontal 18

Figure 21 Muffle Furnace used for heat treatment, Samples after Heat treatment....................... 19

Figure 22 Tensile test-C-11000 20

Figure 23 Spec Sheet C-11000 [15] 21
Figure 24 Tensile test Cu As Sprayed (H) 22
Figure 25 Tensile test Cu-As sprayed (E) 23
Figure 26 Tensile test Cu-As sprayed (V) 24
Figure 27 Tensile test Cu-400C heat treat (compiled) 25
Figure 28 Tensile test 600C heat treat compiled 26
Figure 29 Schematic of SPT [2] 27
Figure 30 Schematic of the shear deformation (a) pure shear and (b) with bending of the blank material fibers [18] 28
Figure 31 SPT C-11000 29
Figure 32 SPT Cu As Sprayed (H) 29
Figure 33 SPT Cu As Sprayed (E) 30
Figure 34 SPT Cu As Sprayed (V) 30
Figure 35 SPT Cu-400C heat treat (compiled) 31
Figure 36 SPT Cu-600C heat treat (compiled) 31
Figure 37 Co-relation between UTS and USS for As sprayed copper 33
Figure 38 Co-relation of UTS and USS for Heat-treated copper 33
Figure 39 Conductivity Cold-Sprayed Cu 34
Figure 40 Vickers hardness (0.3gF) 35
Figure 41 Interactions of Electrons with matter [21] 36
Figure 42 SEM Wrought Copper C-11000 BSE Mode
Figure 43 SEM Wrought Copper C-11000 SE Mode 37
Figure 44 SEM As Sprayed Horizontal BSE mode
Figure 45 SEM As Sprayed Horizontal SE mode 37
Figure 46 SEM As Sprayed Edge BSE Mode
Figure 47 SEM As Sprayed Edge SE Mode 37
Figure 48 SEM As Sprayed Vertical BSE Mode
Figure 49 SEM As Sprayed vertical SE Mode 38
Figure 50 SEM 400C Heat treated Cu BSE Mode
Figure 51 SEM 400C Heat Treated Cu SE Mode 38
Figure 52 SEM 600C Heat Treated Cu BSE Mode

Figure 53 SEM 600C Heat Treated Cu SE Mode 38
Figure 54 SEM SPT Crack As Sprayed Horizontal BSE Mode
Figure 55 SEM SPT Crack As Sprayed Horizontal mode 39
Figure 56 SEM SPT Crack As Sprayed Edge BSE Mode
Figure 57 SEM SPT Crack As Sprayed Edge SE mode 39
Figure 58 SEM SPT Crack As Sprayed Vertical BSE Mode
Figure 59 SEM SPT Crack As Sprayed Vertical SE Mode 40

List of Tables

Table 1 Dimensions of the Dog-bone used for tension tests [9] 13

Table 2 Compiled Data C-11000 Tension test 21

Table 3 Compiled Data Cu-As sprayed (H) Tension test 22

Table 4 Compiled Data Cu-As sprayed (E) Tension test 23

Table 5 Compiled Data Cu-As sprayed (V) Tension test 24

Table 6 Compiled Data 400C heat treat tension test 25

Table 7 Compiled Data 600C heat treat tension test 26

Table 8 Compiled Data for Co-relation of SPT and tensile test 32

Table 9 Electrical Conductivity compiled 34

Table 10 Vickers Hardness compiled 35

Abstract

Mechanical properties of a material always play a key role in identifying its application. The mechanical properties of metals determine the range of usefulness of a material and establish the service life that can be expected. Stronger the material; more likely it is to be used in a heavy-duty environment. Mechanical properties are also used to help classify and identify material. The common properties evaluated are strength, ductility, hardness, impact resistance, and fracture toughness. There are various tools available today to evaluate the mechanical properties of a material; typically; Tensile strength using the UTM; hardness using Vickers, Rockwell etc. hardness tester, Electrical conductivity of metals using C-AFM / eddy current conductivity method etc. Thermal spray is one of the emerging industries in the field of additive manufacturing. Variation in properties are most likely to occur in Additive-manufacturing parts. It is thus necessary to establish a quality control. At the same time this quality control method should be economical (low experimental cost; minimum material wastage), time-saving.

The study aims to establish a correlation between the tensile strength and shear strength of Cold-sprayed (Thermal spray) Cu using miniaturized SPT. Cold sprayed samples were manufactured in collaboration with Spee3D (an Australian based company) [3]. An attempt has been made to establish SPT as a quality control tool for materials with limited availability. Wrought copper C11000 (H-4 temper) has been used as a baseline for comparison. Characterization using SEM and other mechanical properties viz, Hardness and electrical conductivity are measured.

Chapter 1
Introduction

1.1 Introduction to Additive Manufacturing

Additive **M**anufacturing (**AM**) is a comprehensive term to describe the technologies/processes that build 3D components by adding a layer of material at each step; the materials being plastics, polymers, metals etc. A usual platform for the AM techniques is the use of a computer, a CAD software, machine equipment and a layering material. The AM machine reads the CAD file keeps on adding layers of material to make a 3D object. [5]

The term **AM** encompasses many technologies like 3D Printing, Rapid Prototyping (RP), Direct Digital Manufacturing (DDM), layered manufacturing, thermal sprays etc. Thermal sprays is one of the conventional/traditional AM techniques which does not involve any CAD platforms.

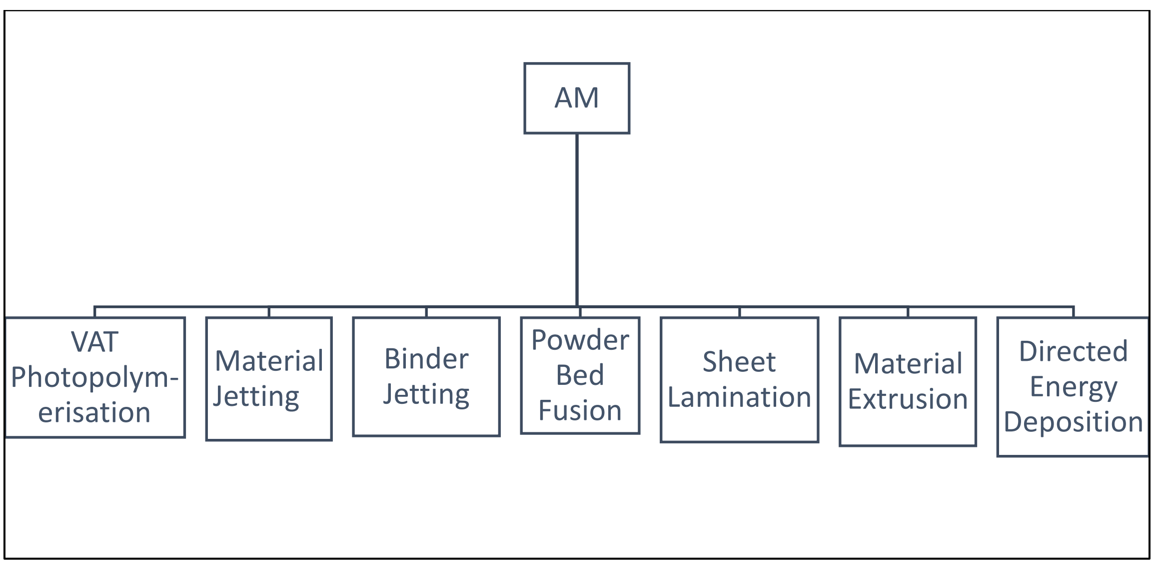

Figure 1 Types of AM Techniques [5]

The above block diagram enlists the various AM techniques existing till date. Every technique has some process variation for eg: type of deformation (plastic etc.); process temperature (melting /non- melting) [6]

1.2 Limitation in Additive Manufacturing

Although AM has many advantages; the current research industry is striving to prove this concept economically viable in-order to replace the conventional manufacturing methods viz, casting forging etc. Limitations also include the complexity of the components to be manufactured. Complexity and Geometric dimensions directly relate to the development cost. The AM components also have a huge variation especially for thermal sprays. In-order to make this technology commercially viable for 3D printing; these variations should be easily detected and minimized. Thus, this escalates to establish a quality control in-order to determine the technical quality (in terms of strength and other mechanical properties) in-order to make improvements in the material.

1.3 Cold Spray Technology

Cold spray is one of the thermal spray technologies which unlike other thermal sprays is a solid-state process. It uses gas to accelerate powder particles at supersonic velocity to impact on the substrate to form a coating [4]. The process temperature is always below the melting temperature of the metal powder to be bombarded. Hence the name. A high-pressure gas (usually Nitrogen or Helium) accelerates metal powder particles to a supersonic gas velocity helping the powder particles to plastically deform on the substrate thereby forming a coating [7].

The cold spray system usually comprises of components such as nozzle, heater, powder feeder and an air compressor supply. The figure below is a visual representation of the process.

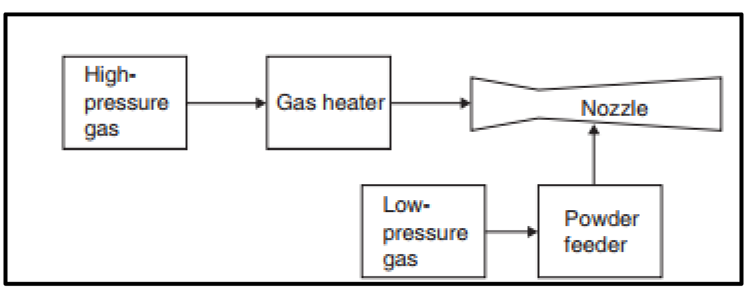

Figure 2 Cold Spray Process Block Diagram [4]

The process map goes as follows:

An inert gas (helium/nitrogen) is compressed to a high pressure (typically 500 psi +) and heated to a temperature around 500-600C. This is allowed to pass through a convergent-divergent type nozzle also known as De-Laval nozzle. At the same time the same inert gas (precursor) is passed through the powder feeder and let into the nozzle (usually prior to the throat)

High velocity is achieved due at the expansion area of the nozzle where a certain pressure drop is also observed. This velocity being more than the critical velocity; it escalates the powder particles to hit on the substrate and thus stick on the substrate due to plastic deformation. Once the initial layer is formed; subsequent layers are formed on the initial coated layer.

The bond strength of the coating completely depends upon the initial few layers. Greater the bond; the coating can be used in heavy duty applications.

***The parameters above are pertained to a specific application used for this study. They can vary as per application.**

Chapter 2
Aim and Scope for the Research

2.1 Aim

Quality control of thermal sprays as well as other AM techniques is turning out to be one of the necessities to lead the AM industry to supersede the conventional manufacturing methods (viz, casting, forging etc.) The aim of this study is to establish a linear correlation between tensile strength and shear strength of cold-sprayed copper samples using miniaturized shear punch test [2]. An attempt for linear correlation for wrought alloys has already been made by a few researchers [2] [8]. This study extends the attempt for cold-sprayed copper. The tensile strength of any material is usually determined using UTM. A dog-bone structure must be manufactured as per ASTM E-8/E-8M/16a standard [9]. Manufacturing of these dog bone like structures is usually done on CNC machines which is a time-consuming costly process involving material wastage.

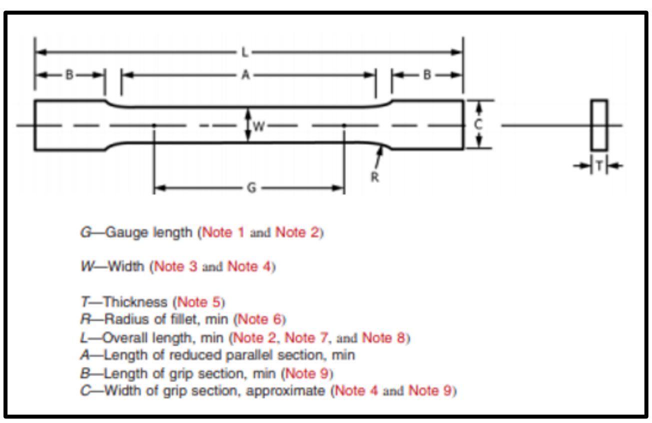

Figure 3 A sample Dog-bone as per ASTM E8 [9]

The figure above is a schematic of the dog-bones usually manufactured for tensile testing. Whereas; for the miniaturized SPT [2], the test sample can be varied with a size within 1inchx1inch and a thickness ranging from 250μm to 1500μm. Compared to the E8 dog bones; the test samples for SPT involve less material and can be precisely manufactured by using methods such as wire EDM etc. Thus, it aids in quick and economic testing.

Apart from a linear correlation between tensile strength and shear strength this study also involves measurement of mechanical properties:

- Hardness (Vickers)
- Electrical Conductivity
- Characterization using SEM images.

The effect of heat treatment of as-sprayed copper with respect to hardness and conductivity has also been observed.

2.2 Scope

The scope of this research is limited to evaluation of mechanical properties for cold-sprayed copper only. The experimental procedure does not include the use of laser systems.

This study also does not include evaluation of properties for other thermal spray or AM techniques.

Chapter 3
Cold spray

Continuing with the principle of working of cold-spray; the quality of the sprayed samples depends upon various parameters. In this section few of such parameters are discussed.

3.1 Particle velocity and temperature

The temperature used in cold spray deposition is always below the melting point of the feedstock powder. Hence the cold spray is a solid deposition process which works on plastic deformation [4].

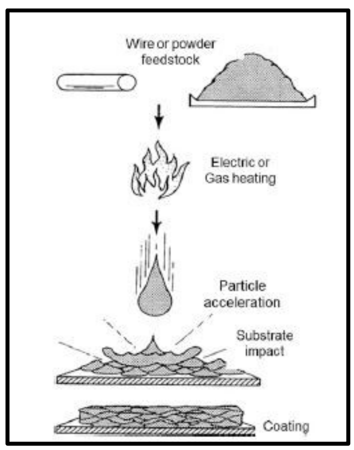

Figure 4 Representation of powder and
Particle acceleration to Coating formation [4]

Particle interaction is affected by the gas media. Usually Nitrogen or Helium are the two medias used. The particles velocity is better in helium than nitrogen due to a high molecular weight.

$$v = (\frac{\gamma RT}{M_w})^{1/2} \quad [4]$$

where,

v is the speed of the sound.

γ is the ratio of the specific heats (1.4 for air and 1.66 for He)?

R is the gas constant (8.314 J/mole-K)

T is the gas temperature in K

M_w is the molecular weight of the gas.

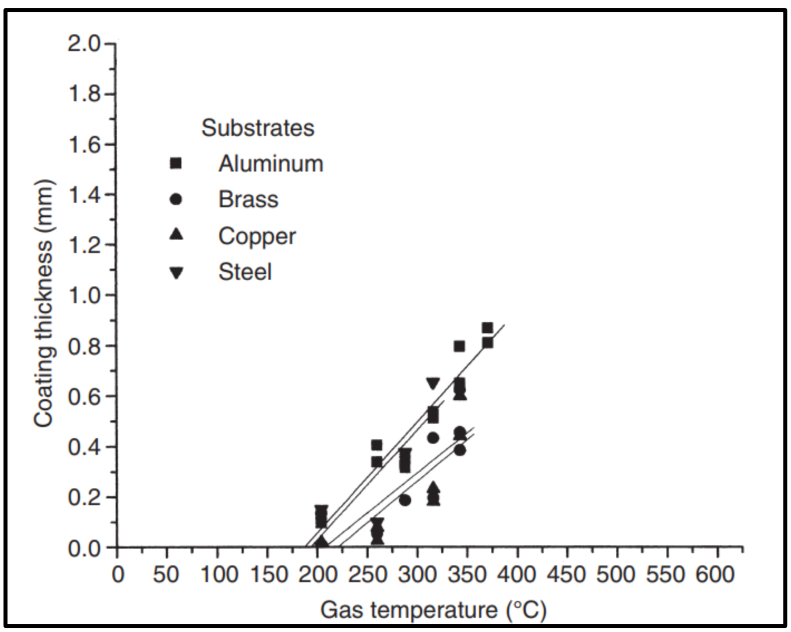

Figure 5 Effect of gas temperature on coating thickness [4]

Parameter	Effect on v_{pi}	Effect on v_{cr}
Particle		
Melting temperature	...	↑
Specific heat	...	↑
Hardness	...	↑
Density	↑↓	↓
Size	↑↓	↓
Gas		
Temperature	↑	↓
Pressure	↑	...
Nozzle		
Length	↑	...

Figure 6 Effect of parameters on Critical velocity and Impact particle velocity [10]

The influence of key material and process parameters on Impact velocity Vpi and Critical velocity Vcr is summarized.

3.2 Nozzle Design

Supersonic flows in fluid dynamics are always obtained using a De-laval Nozzle or a convergent-Barrel nozzle. These are the typical once used in cold-spray technology [11]. The nozzle design directly affects coating quality.

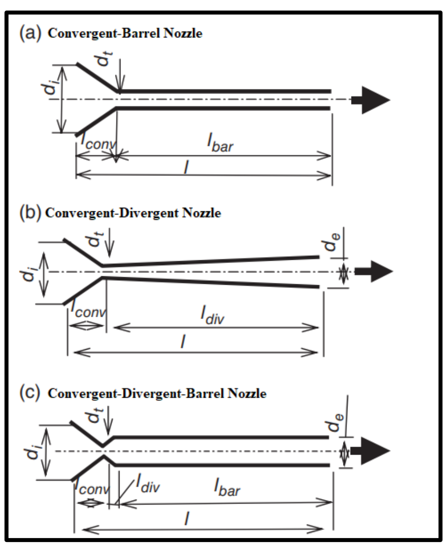

Figure 7 Nozzles used in cold-spray technology [4]

The throat diameter and exit divergence play a major role in the deposition.

The nozzle which we used for this experimental analysis and was designed and developed by the Additive Manufacturing and Processing Laboratory at University of Michigan Dearborn. The nozzle used in our current study was a circular cross sectional shaped nozzle. The nozzle used was a dual feed inlet for powder feeding.

3.3 Bonding Mechanism

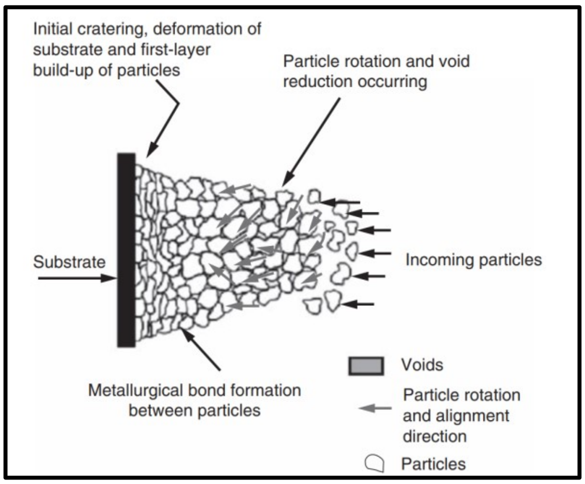

Figure 8 Schematic of Coating Deposition [4]

Adiabatic shear instability [12] is the key phenomena towards the bonding mechanism of cold-spray. For such conditions, the plastic strain energy dissipates as heat increases the temperature, which causes softening of the material. Thus, the rate of strain hardening decreases and the flow stress reaches a maximum value, followed by a monotonic decrease in flow stress with plastic strain [4].

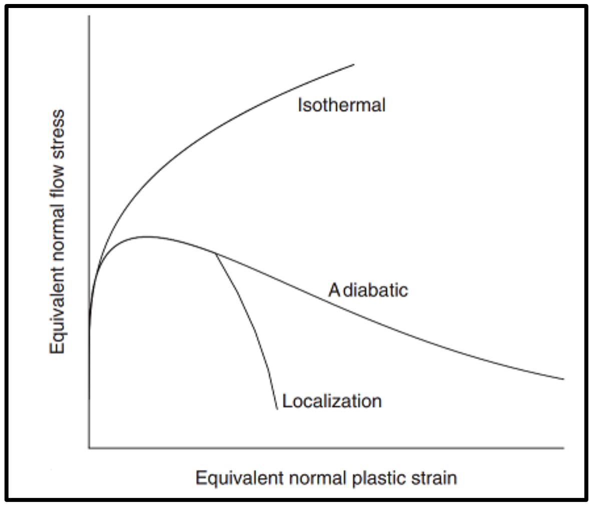

Figure 9 Stress curves for isothermal material, adiabatic material and following an adiabatic shear localization [12]

Fluctuations in stress, strain, temperature or microstructure, and the inherent instability of strain softening, can give rise to plastic-flow (shear) localization. In such cases, shearing and heating (and consequently softening) become localized, while the straining and heating in the surrounding material regions practically stops. This, in turn, causes the flow stress to quickly drop to zero [12].

The particle–particle or particle–substrate interfacial areas experience severe localized shear deformation during impact, which disrupts the thin oxide surface films on the particles, permitting strong particle–substrate contact [12]. These principles and concepts are necessary for bonding.

3.4 Standoff distance

Particle size, density, shockwave determine the standoff distance. The standoff zone has been categorized into three regions. A study has been done by a few researchers [13] previously on the effect of standoff distance on various properties of a cold-sprayed coating. It has been observed that the deposition efficiency was decreased with the increase of standoff distance from a range of 10 mm to 110 mm.

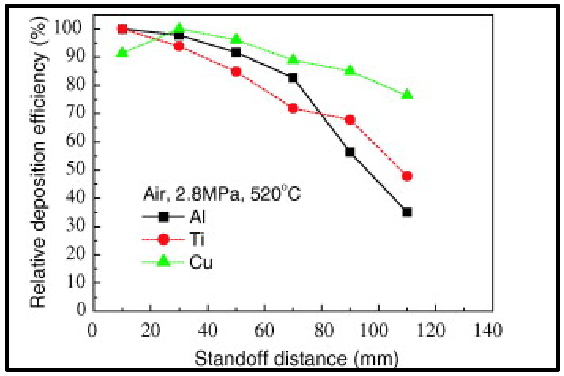

Figure 10 Effect of standoff distance on the calculated gas and Cu particle (40 µm) temperatures close to substrate [13]

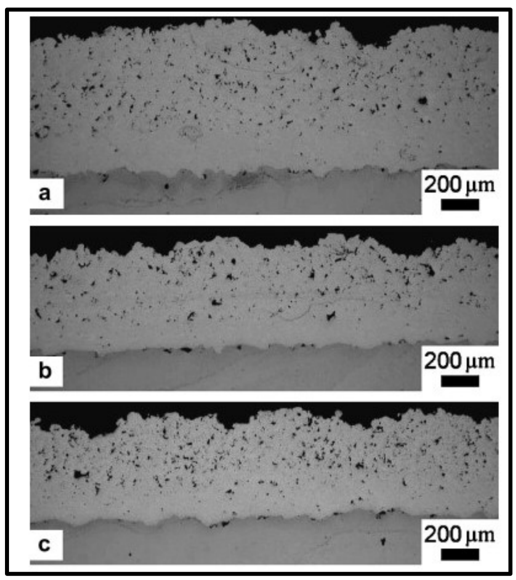

Figure 11 OM images of Al coatings with standoff distances of (a) 10 mm, (b) 30 mm, (c) 50 mm [13]

It has been generalized that for ductile materials like steel, aluminum etc a standoff distance of 10mm leads to a maximum deposition efficiency with a minimum wastage of powders.

Chapter 4
Characterization and Experimental

Characterization and Analysis

All the equipments/instruments used for the study are categorized and mentioned below.

4.1 UTM (Universal Testing Machine)

The Tensile tests and shear punch tests for the study were done on an Instron 5967.

4.1.1 Tensile Tests

The tensile tests on the coatings were done were done at a ramp rate of 1.5mm/min. This value was chosen as per mentioned in the ASTM E8 standard [9].An extensometer (clipped on the dog bone) was used to determine the strain rate.

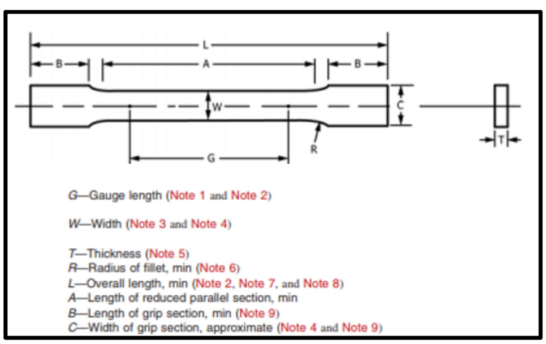

Figure 12 Dog Bone as per ASTM E8 [8]

The dimensions of the dog bones used are as per the table below for a gauge length of 25mm

Title	Abbrv	Dimension
G	Gauge length	25mm
W	Width	6mm
T	Thickness	6mm
R	Radius of Fillet	6mm
L	Overall Length	100mm
A	Length of reduced parallel section, min	32mm
B	Length of gripped section, min	30mm
C	Width of gripped section, min	10mm

Table 1 Dimensions of the Dog-bone used for tension tests [9]

4.1.2 Shear Punch Tests

The sample size used for shear punch test was under a dimension 10mmX10mmX1mm. The ramp rate used for the experiments was 0.5mm/min. This rate was chosen with reference to a previous study [2]. This study also explained that; the thickness of SPT samples has a negligible effect on the shear strength of the material [2]. Hence all the samples of 1mm thickness were used for testing. The samples were cut using a Brother HS-300 wire-edm. All the samples were then polished using a 600grit paper in-order to achieve uniformity in readings.

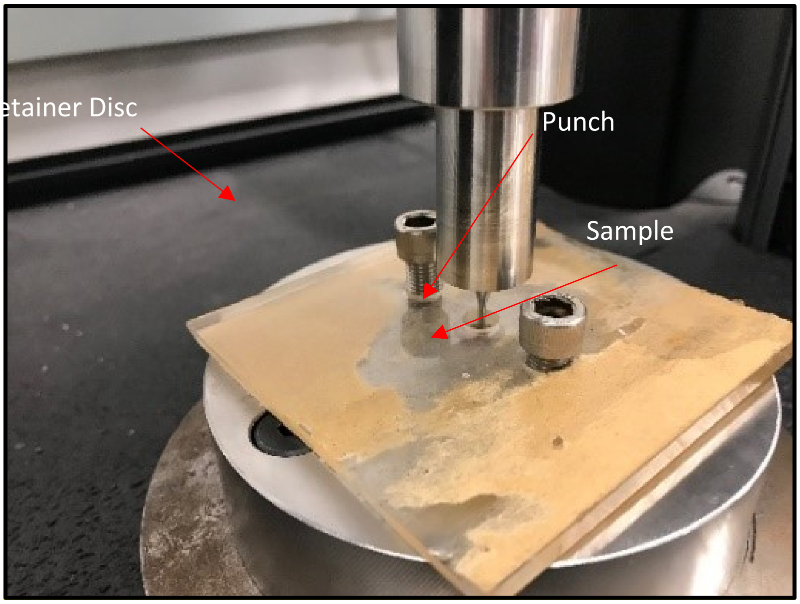

Figure 13 Experimental setup for SPT

4.2 Microstructural Characterization

The amount of the porosity present in the coating is one of the most important criteria for measuring the coating quality. The porosities are caused due to various factors including the coating material and the process conditions. Furthermore, porosities can mostly be associated with the gases such as nitrogen, oxygen and hydrogen which may be liberated due to their reduction in solubility when the temperature decreases from a higher value to atmospheric temperature.

Figure 14 HITACHI Scanning Electron Microscope

Image characterization in this study was done using the Scanning electron microscope. The Scanning electron microscope works on the principle that electrons interact with the atoms in the workpiece to produce Secondary Electron (SE) and Back Scattering Electron (BSE) which are detected and captured with the desired detectors. The SEM used for our current study is HITACHI Scanning Electron Microscope (SEM)(Model S-2600N,University of Michigan Property 374500) . The images used in the current study are Back Scattered Electron (BSE) as well as Secondary electron(SE) images for the coatings.

Standard Metallographic procedures were followed to prepare the samples. Mounts were prepared using an Epomer epoxy on a Buehler mounting press.

4.3 Vickers Hardness

Figure 15 Vickers Hardness Tester

Hardness readings were taken using a Struers Vickers Hardness tester in the figure above. A constant load of 300g was applied for 10secs.

4.4 Electrical Conductivity

Figure 16 Eddy-current Conductivitymeter

Figure 17 Measurement done on a sample copper bar

The electrical conductivity of the cold-sprayed copper samples was measured using an eddy-current conductivity meter. Eddy-current measurement is a non-destructive test. The probe is placed on the sample for measurement. For non- magnetic materials; the change in impedance of the material can directly be correlated to the change in electrical conductivity [14]. These instruments measure the value in terms of %IACS (International Annealed Copper Standard) or MS/m. All the measurements are relative to a benchmark cooper sample which is considered as highly conductive (100%IACS). The measurements were taken both in %IACS and MS/m. For this method as the conductivity can vary at every point; several readings were taken followed by a statistical analysis.

Chapter 5
Results and Discussion

5.1 Cold-Spray

Experiments were carried out using the system developed at the AMPL (additive Manufacturing process laboratories) at the U of M-Dearborn in collaboration with Spee3D who are working on commercializing the 3D printing technology. A low pressure cold spray system has been used which helps in achieving a good quality coating with relative low and economic gas condition.

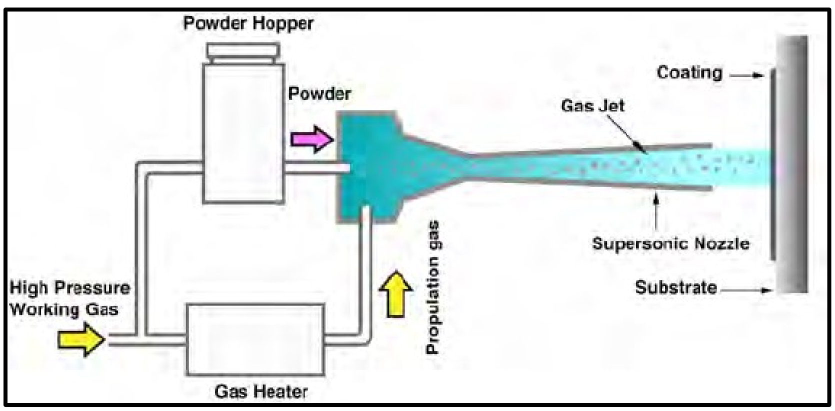

Figure 18 Typical Cold Spray System [4]

The experiments also use a specially designed de-laval nozzle (circular profile) with dual feed powder inlet at University of Michigan Dearborn. The scheme of the powder injection was done downstream. Samples were sprayed in 3 different orientations on an Al6061 substrate. Different orientations were used to check if the amount of buildup layer affects the mechanical properties of the material. This judgement shall be beneficial for applications like 3-D printing.

In-order to restrict a variable and conduct a systematic experiment; same parameters were used for all the cold-sprayed copper samples with different orientations.

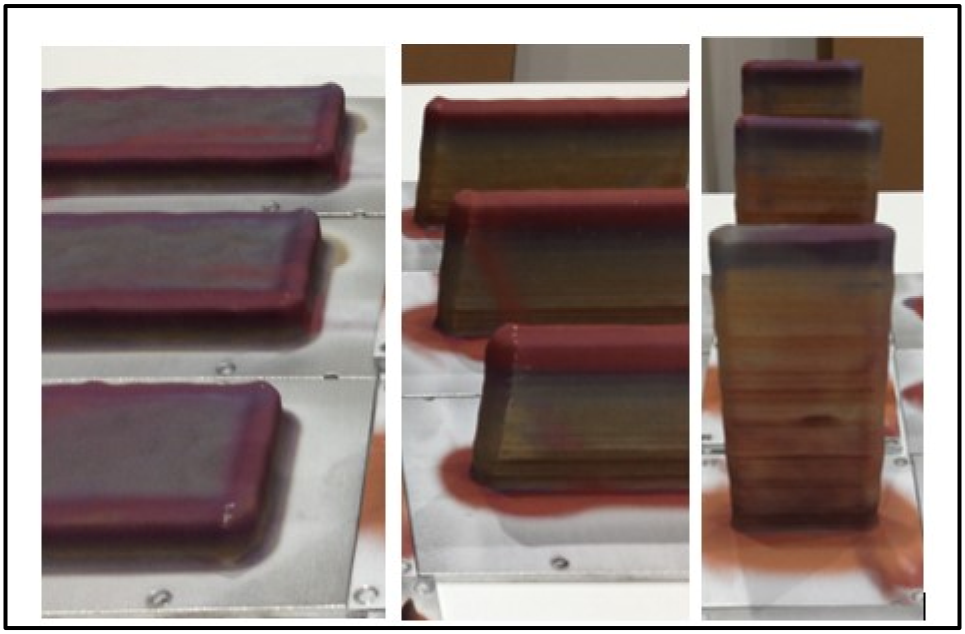

Figure 19 Sprayed Copper Coatings on 6061 substrates manufactured at Spee3D L to R Horizontal, Edge, Vertical

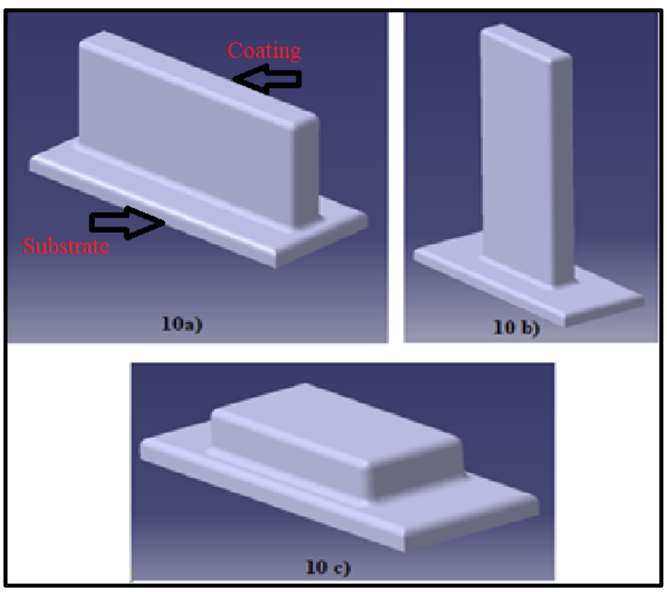

Figure 20 CAD representation a) Edge b) Vertical c) Horizontal

Following parameters were used for the spray experiments: -

- Nozzle profile: - Circular (X2)
- Main Gas pressure 32 Bar

- Carrier gas Flow 34scfm
- Process temperature- 500C
- Powder Flow = 20g/min
- Powder Type = >99.5% Cu @ 20um nominal i.e D90=20um
- Substrate used: - Al 6061

Dog Bones and test samples were manufactured from these sprayed samples. 3 samples of each orientation and each HT temp were used.

5.2 Heat Treatment

In order to analyze the effect of temperature (annealing); one batch was heat treated at 400C for 4 hours and other at 600C for 4 hours in a muffle furnace. During heat treatment the aluminum substrates were chopped-off to avoid meltdown at high temperatures.

The heat treatment was done in the presence of air media (closed). The samples were also air-cooled inside the furnace.

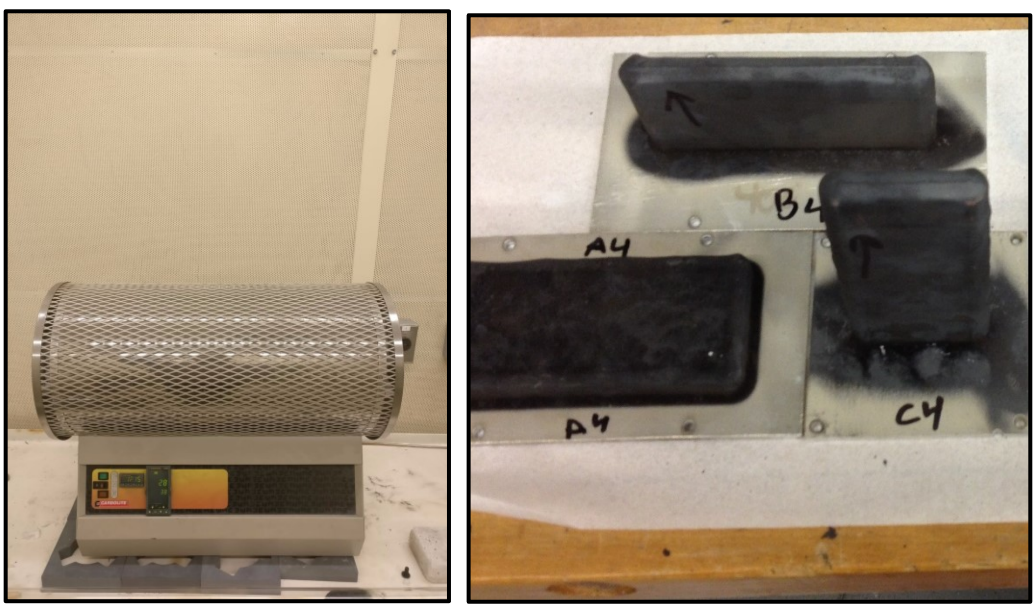

Figure 21 Muffle Furnace used for heat treatment, Samples after Heat treatment.

5.3 Design of Experiments

- No. of Orientations: - 3 (Horizontal, Vertical, Edge)
- Heat Treat parameters: - 3 (As sprayed, 400C, 600C)
- Replicates: - 3
- Total no. of runs: - 27

5.4 Tensile Tests

As mentioned above dog-bones were manufactured from the sprayed coatings with 3 different orientations(Horizontal,Edge,Vertical) and 3 different heat treatments (As sprayed, 400C, 600C).

5.4.1 Cu-11000

For establishing a baseline for the experiment; wrought copper C-11000 (Hard temper/H4 temper code) was used [15]. The wrought bar was procured directly from McMaster Carr [16].

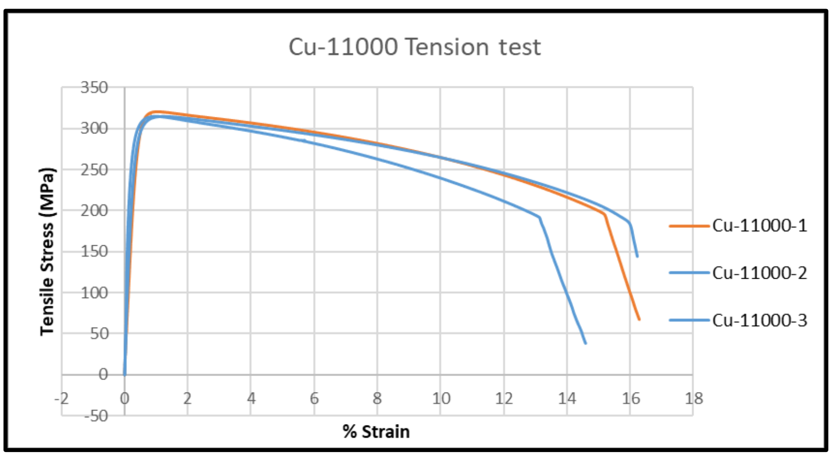

Figure 22 Tensile test-C-11000

The following table shows the compiled data for the experiment. The data corresponds to statistical value of 3 dog bones of C-11000(H4):

Title	Mean Value	Std.Dev
Max Load	12570.03 N	130.94
UTS	316.705 MPa / 45.93 ksi	3.299 MPa / 0.478 ksi
Yield	297 MPa / 43.07 ksi	8.18 MPa / 1.186 ksi
Youngs Modulus	115570.76 MPa /16762 ksi	2344.86 MPa/ 340.093 ksi
Elongation	15.7 %	0.96 %

Table 2 Compiled Data C-11000 Tension test

The resulting values were matching to the standard specification certificate [15] received with the procured stock; thus, setting a benchmark for the experimentation procedure.

C11000*

Tradename: Electrolytic Tough Pitch
Designation: ETP
Type: Wrought
Class: COPPERS, Coppers

Chemical Composition

	Element
	Cu(1,2,3)
Min (%)	99.90

(1) Oxygen and trace elements may vary depending on the process.
(2) This is a high conductivity copper which has, in the annealed condition a minimum conductivity of 100% IACS.

Mechanical Properties*

Form	Temper	Temper Code	Tensile Strength (ksi)	YS-0.5% Ext (ksi)	Elongation (%)	Rockwell B scale	Rockwell F scale	Rockwell 30T scale	Shear Strength (ksi)	Torsion Modulus (ksi)	Izod (ft-lbs)	Fatigue Strength** (ksi)	Ultimate Tensile Strength in Shear (ksi)	Section Size (in)	Cold Work (%)
Flat Products	1/2 Hard	H02	42 Typ	36 Typ	14 Typ	40 Typ	84 Typ	50 Typ	26 Typ			13 Typ		0.04	
	1/4 Hard	H01	38 Typ	30 Typ	35 Typ	25 Typ	70 Typ		25 Typ				25 Typ	0.025	
		H01	38 Typ	30 Typ	25 Typ	25 Typ	70 Typ	36 Typ	25 Typ					0.04	
	1/8 Hard	H00	36 Typ	28 Typ	40 Typ	10 Typ	60 Typ		25 Typ					0.025	
		H00	36 Typ	28 Typ	30 Typ	10 Typ	60 Typ	25 Typ	25 Typ					0.04	
	As Hot Rolled	M20	32 Typ	10 Typ	50 Typ		40 Typ		22 Typ					0.025	
		M20	34 Typ	10 Typ	45 Typ		45 Typ		23 Typ					0.04	
	Extra Spring	H10	57 Typ	53 Typ	4 Typ	62 Typ	95 Typ	64 Typ	29 Typ					0.04	
	Hard	H04	50 Typ	45 Typ	12 Typ								28 Typ	0.24	
		H04	50 Typ	45 Typ	6 Typ	50 Typ	90 Typ	57 Typ	28 Typ				28 Typ	0.04	
		H04	45 Typ	40	20 Typ	45 Typ	85 Typ		26 Typ					1	

Figure 23 Spec Sheet C-11000 [15]

5.4.2 Copper As Spray

5.4.2.1 Copper-AS-Horizontal Orientation

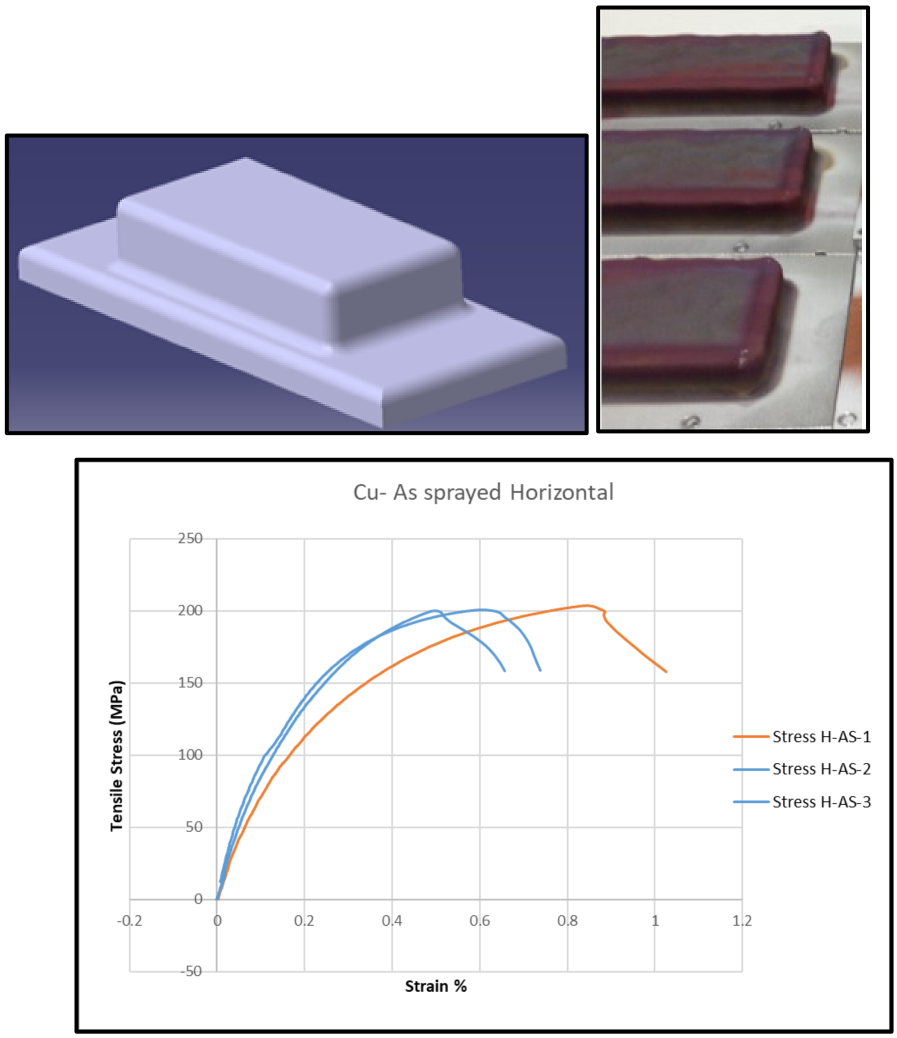

Figure 24 Tensile test Cu As Sprayed (H)

Title	Mean Value	Std.Dev
Max Load	7993.95 N	82.7 N
UTS	201.41 MPa / 29.21 ksi	2.083 MPa / 0.302 ksi
Yield	169 MPa / 24.51 ksi	13.89 MPa / 2.01 ksi
Youngs Modulus	99346.33 MPa /14408 ksi	4438.74 MPa / 643.78 ksi
Elongation	0.8 %	0.19 %

Table 3 Compiled Data Cu-As sprayed (H) Tension test

5.4.2.2 Copper-AS-Edge Orientation

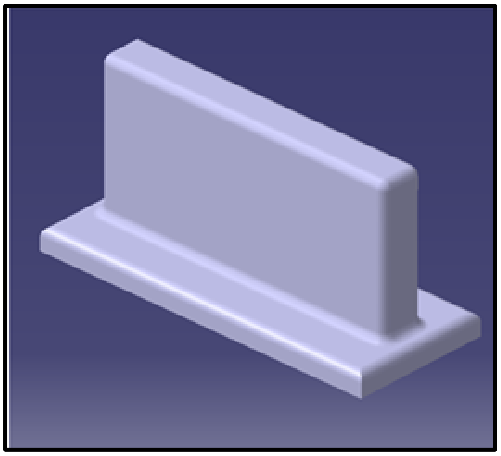

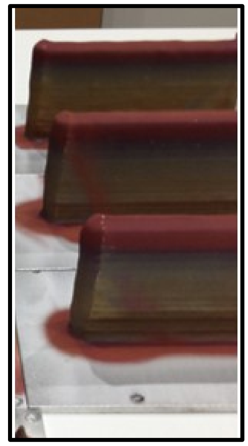

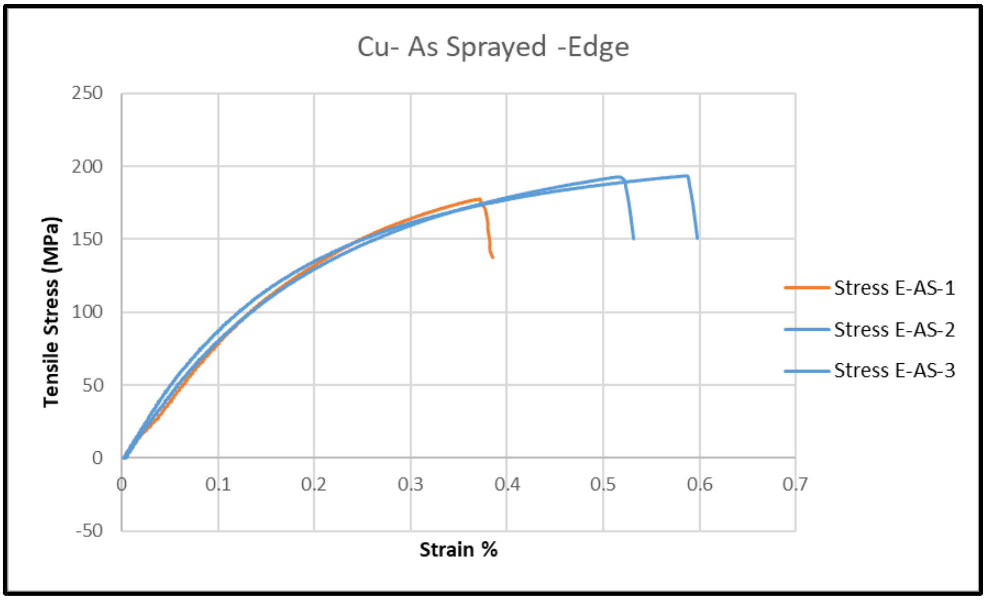

Figure 25 Tensile test Cu-As sprayed (E)

Title	Mean Value	Std.Dev
Max Load	7457.32 N	278.93 N
UTS	187.889 MPa / 27.25 ksi	7.02 MPa / 1.018 ksi
Yield	172 MPa / 24.94 ksi	4.96 MPa / 0.71 ksi
Youngs Modulus	88249.33 MPa /12799.48 ksi	5227.09 MPa/ 758.125 ksi
Elongation	0.5 %	0.08 %

Table 4 Compiled Data Cu-As sprayed (E) Tension test

5.4.2.3 Copper-AS-Vertical Orientation

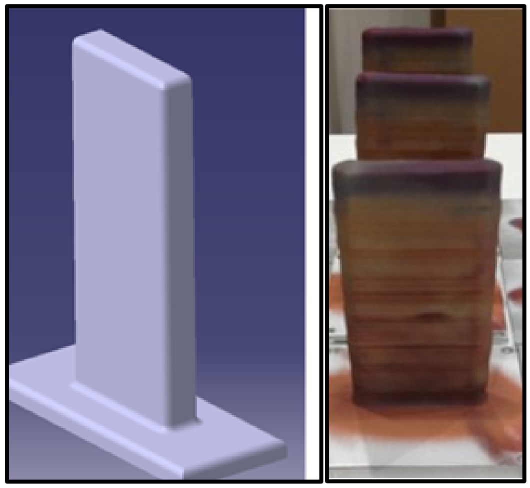

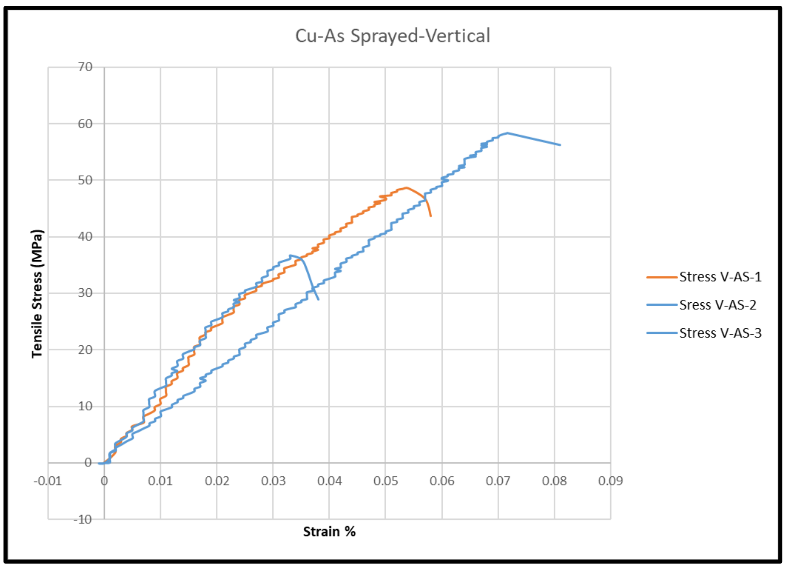

Figure 26 Tensile test Cu-As sprayed (V)

Title	Mean Value	Std.Dev
Max Load	1901.92 N	430.86 N
UTS	47.91 MPa / 6.94 ksi	10.85 MPa / 1.57 ksi
Yield	46 MPa / 6.67 ksi	10 MPa / 1.45 ksi
Youngs Modulus	107070.33 MPa /15529.19ksi	16815.256 MPa /2438 ksi
Elongation	0.05 %	0.02 %

Table 5 Compiled Data Cu-As sprayed (V) Tension test

5.4.3 Copper 400C heat-treat

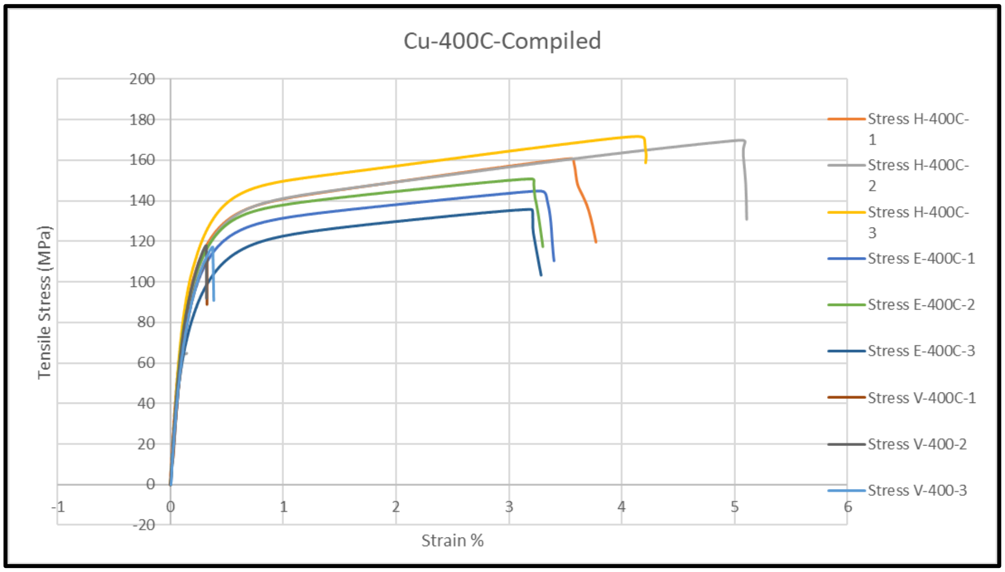

Figure 27 Tensile test Cu-400C heat treat (compiled)

Horizontal			Edge			Vertical		
Title	Mean Value	Std.Dev	Title	Mean Value	Std.Dev	Title	Mean Value	Std.Dev
Max Load	6648.39	230.56	Max Load	5708.282	300.86	Max Load	4596.4088	120.846
UTS	167.5	5.8	UTS	143.82	7.58	UTS	115.8073	3.04
Yield	124.33	5.131	Yield	111.66	10.4	Yield	100	5
Youngs Modulus	86448.33	2144.06	Youngs Modulus	87914	466.50	Youngs Modulus	81048	3781.49
Elongation	4.36	0.68	Elongation	3.32	0.06	Elongation	0.342	0.036

Table 6 Compiled Data 400C heat treat tension test

5.4.4 Copper 600C heat-treat

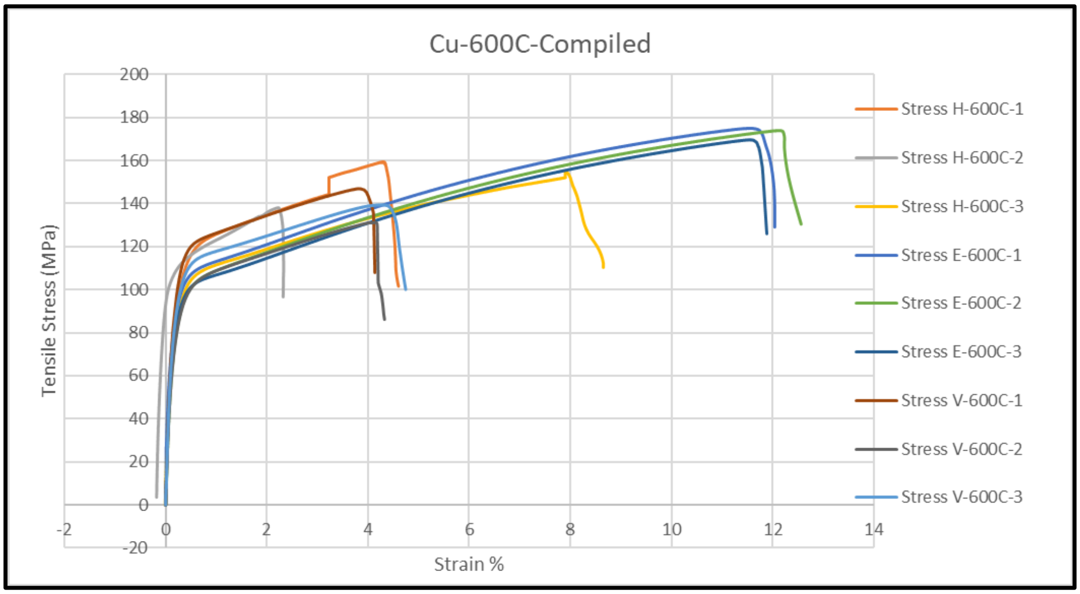

Figure 28 Tensile test 600C heat treat compiled

Horizontal			Edge			Vertical		
Title	Mean Value	Std.Dev	Title	Mean Value	Std.Dev	Title	Mean Value	Std.Dev
Max Load	5997.38 N	453.76	Max Load	6861.203	112.235	Max Load	5526.91	309.86
UTS	151.105	11.43	UTS	172.86	2.82	UTS	139.25	7.807
Yield	105.66	11.59	Yield	96	1.732	Yield	103.33	7.02
Youngs Modulus	99209	4364.27	Youngs Modulus	95937.3	18216.5	Youngs Modulus	87495.66	6812.26
Elongation	5.185	0.68	Elongation	12.16	0.354	Elongation	4.402	0.311

Table 7 Compiled Data 600C heat treat tension test

5.5 Shear Punch Tests

SPT is quick tool established by many researchers [8] to measure mechanical properties of a material. Dies and punches were procured from Pivot precision tools. [17]

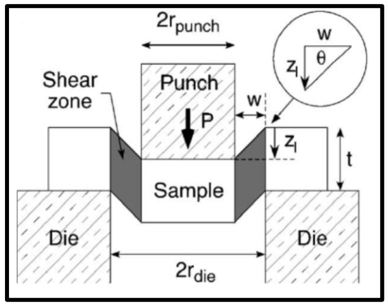

Figure 29 Schematic of SPT [2]

The shear strength of the material is calculated using the following formula where;

P: load applied on UTM

r: Avg. radius $\{(r_{punch} + r_{die})/2\}$ Ravg= 0.84mm

t: Thickness of Sample (1.1mm)

$$\tau = \frac{P}{2\pi r_{avg} t}$$

A graph of load vs Punch Displacement is plotted for the experimental data. This then translates to the shear strength according to the above relation.

The Die and punches used were made of hardened steel (RC 58). Punch die clearance was 15µm.

$r_{punch} = 0.8325$mm $r_{die} = 0.8475$mm

The specimen thickness and strain rate were chosen based on the earlier studies conducted by Guduru et al [2]. According to that study; the sample thickness doesn't affect the shear strength to a greater extent. Also if the punch and die clearance is beyond a certain range the operation results in deep drawing instead of shearing. A punch die clearance of approx. 15μm is maintained in this experimentation.

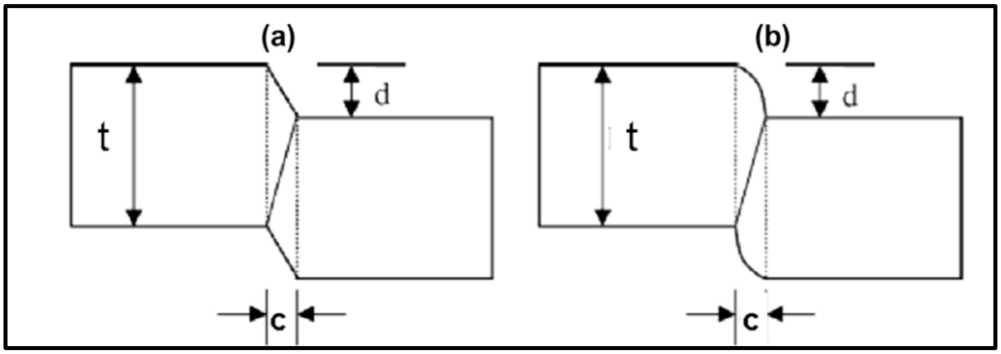

Figure 30 Schematic of the shear deformation (a) pure shear and (b) with bending of the blank material fibers [18]

5.5.1 Cu-11000

For establishing a baseline for the experiment; wrought copper C-11000 (Hard temper/H4 temper code) was used [15]. The wrought bar was procured directly from McMaster Carr [16]. The average shear strength value was similar to the spec sheet [16] of the procured material; thus, calibrating the experiment.

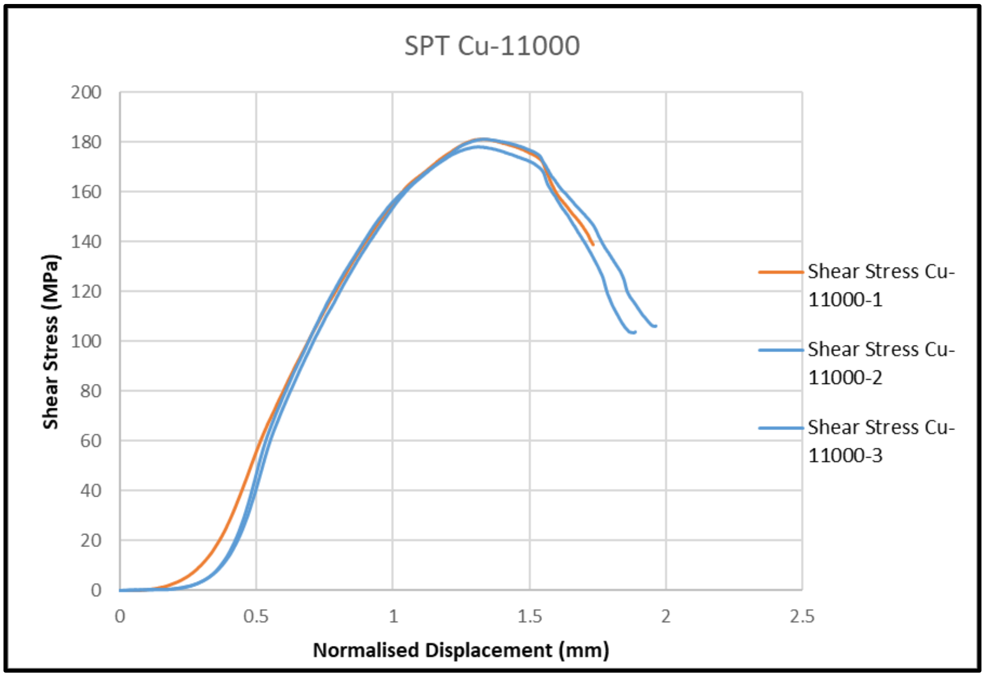

Figure 31 SPT C-11000

USS mean= 180.103MPa Std. dev=1.913 MPa

5.5.2 Copper As Spray

5.5.2.1 Copper-AS-Horizontal Orientation

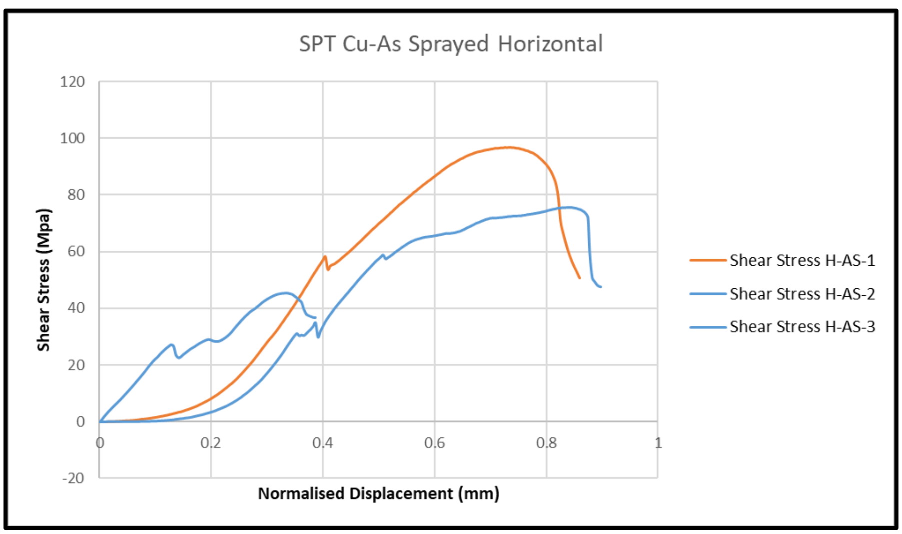

Figure 32 SPT Cu As Sprayed (H)

USS mean= 86.165 MPa Std. dev=14.95 MPa

5.5.2.2 Copper-AS-Edge Orientation

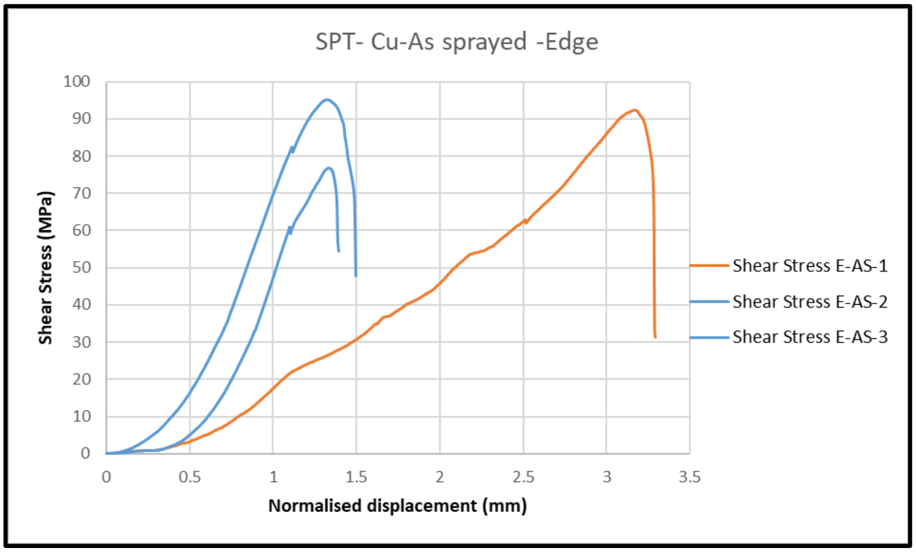

Figure 33 SPT Cu As Sprayed (E)

USS Mean= 87.06 MPa Std. dev=9.43 MPa

5.5.2.3 Copper-AS-Vertical Orientation

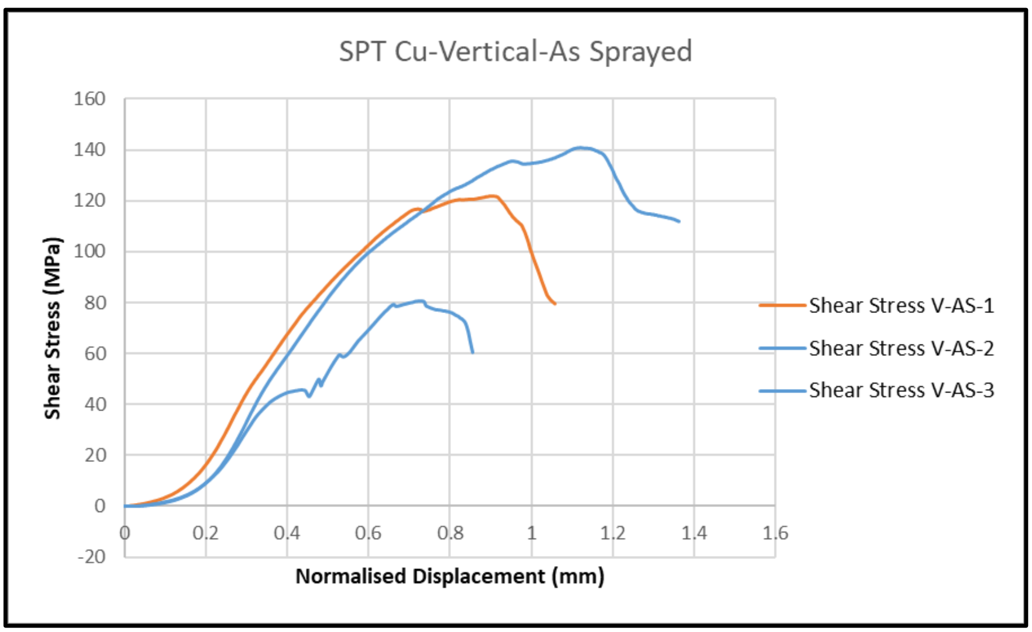

Figure 34 SPT Cu As Sprayed (V)

USS Mean=131.26MPa Std. dev=30.7 MPa

5.5.3 Copper 400C heat-treat

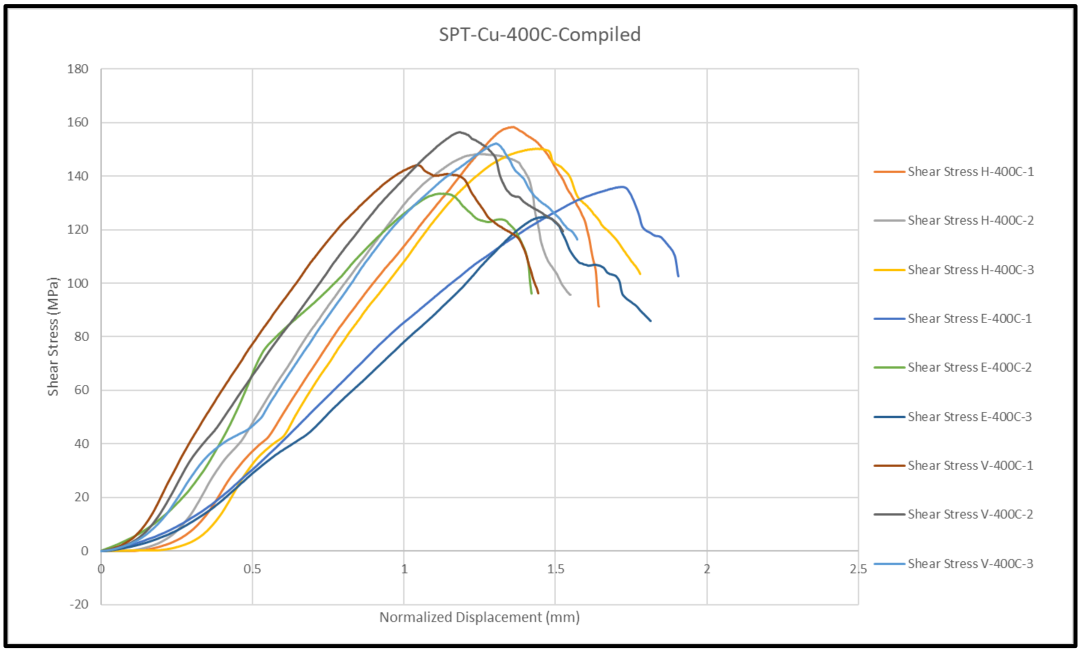

Figure 35 SPT Cu-400C heat treat (compiled)

5.5.4 Copper 600C heat-treat

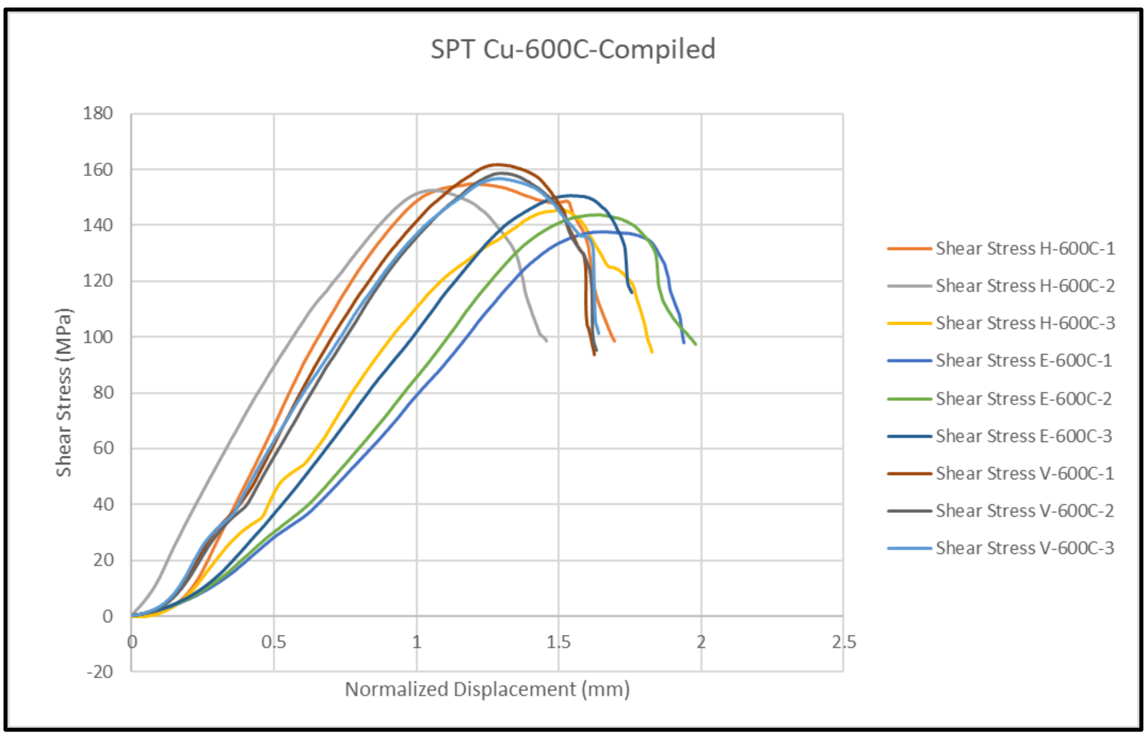

Figure 36 SPT Cu-600C heat treat (compiled)

It was observed from the shear strength curves that heat treatment made the coatings homogenous (approximately equal shear strengths for all orientations.)

5.6 Co-relation of SPT and Tensile test

		Base	Horizontal			Edge			Vertical		
		C-11000	**AS**	**400C**	**600C**	**AS**	**400C**	**600C**	**AS**	**400C**	**600C**
UTS	Mean	316.7	201.41	167.5	151.105	187.889	143.82	172.86	**47.91**	115.8	139.25
	Std. Dev	3.299	2.083	5.8	11.43	7.02	7.58	2.82	5.3	3.04	7.807
USS	Mean	180.103	86.165	152.228	151.029	87.06	131.34	144.12	**131.26**	150.897	159.09
	Std. Dev	1.913	14.95	5.259	4.82	9.43	4.815	6.48	30.7	5.08	2.56

Table 8 Compiled Data for Co-relation of SPT and tensile test

To establish a reference for the experiment; shear punch test was carried out with reference wrought copper [16]. According to a previous study by a few researchers a correlation has been established for wrought materials. It suggests that UTS=1.8*USS [2]

Based on this benchmark; rest of the experiments were carried out. The wrought copper C-11000 happened to follow the same co-relation as mentioned above.

Co-relation was plotted for 2 categories; As sprayed and Heat treated (both temperatures combined).

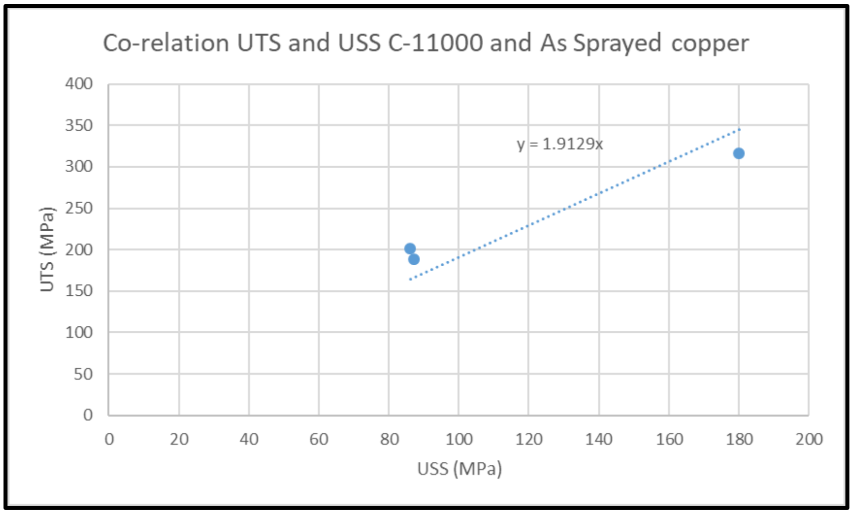

Figure 37 Co-relation between UTS and USS for As sprayed copper

The data points seemed to follow a co-relation of UTS=1.9*USS for Pure Copper C-11000 and As sprayed Copper (horizontal orientation and edge orientation). The Vertical orientation didn't seem to follow a correlation. It is suspected that the mechanical properties (strength) would be low as the build-up layer increases.

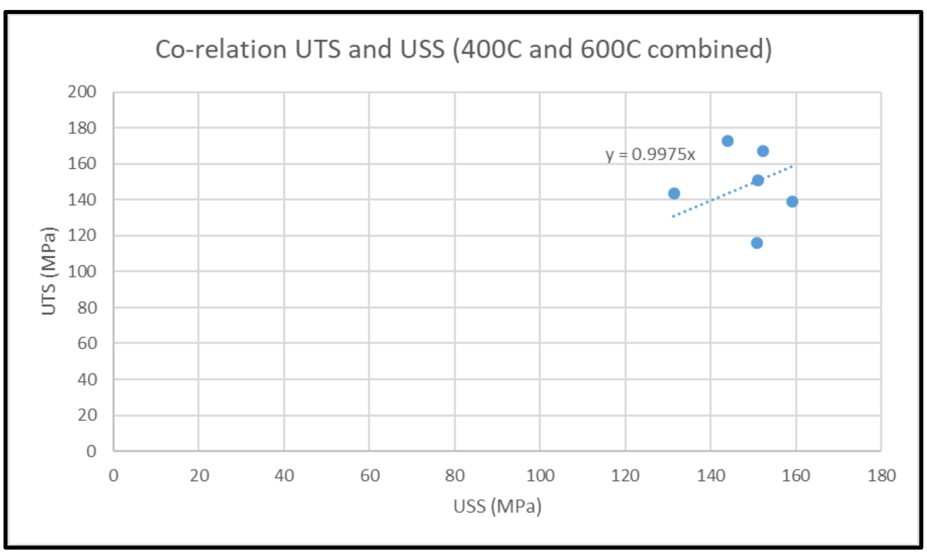

Figure 38 Co-relation of UTS and USS for Heat-treated copper

The data points followed a co-relation of UTS=0.99*USS for all heat-treated cold sprayed copper samples.

5.7 Electrical Conductivity

Conductivity is always measured with respect to pure copper according to a defined standard called International Annealed Copper Standard [1] often expressed in terms of percentage. (%IACS).

Electrical Conductivity was measured for every orientation and heat treat condition. It was observed that conductivity significantly improved with heat treatment. The orientation didn't appear to affect the conductivity but was significantly more than that in the as sprayed samples. C-11000 displayed a 98.5% IACS.

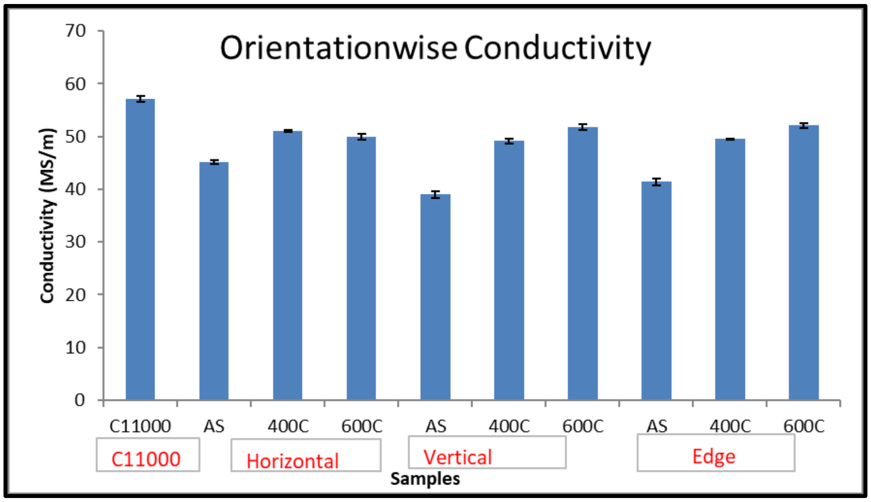

Figure 39 Conductivity Cold-Sprayed Cu

		Horizontal			Vertical			Edge		
	C11000	AS	400C	600C	AS	400C	600C	AS	400C	600C
	57.2	45.4	51.2	49.8	39.6	49.5	52.6	40.5	49.4	52
	58	45	50.9	50.8	38.9	49.7	51.6	41.6	49.5	52.9
	57	45.6	51.4	49.8	38	48.8	51.2	42.2	49.6	51.8
	56.6	44.5	51	49.9	39.3	48.6	52.3	41.4	49.7	52
	56.9	45.2	50.8	49.5	39.2	49.3	51.5	41.2	49.4	51.9
Mean	57.14	45.14	51.06	49.96	39	49.18	51.84	41.38	49.52	52.12
Stdev	0.53	0.42	0.24	0.49	0.61	0.47	0.59	0.62	0.13	0.44
%IACS	**98.52**	**77.82**	**88.03**	**86.14**	**67.24**	**84.79**	**89.38**	**71.34**	**85.38**	**89.86**

Table 9 Electrical Conductivity compiled

5.8 VickersHardness

Vickers hardness was measured with a load of 300gF for 10 secs. The As sprayed coatings displayed approximately same hardness along all orientations and the value was similar to wrought copper C-11000. Heat treatment significantly softened the material and reduced the hardness to as low of 592 MPa. Hardness decreases with the annealing temperature. High amount of dissolved oxygen can be attributed to the change in hardness [19].

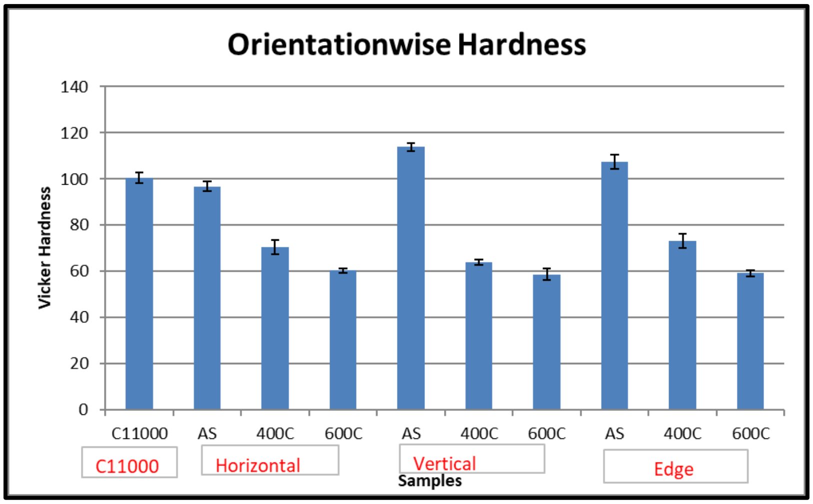

Figure 40 Vickers hardness (0.3gF)

	C11000	**Horizontal**			**Vertical**			**Edge**		
		AS	**400C**	**600C**	**AS**	**400C**	**600C**	**AS**	**400C**	**600C**
	98.9	98.9	68.7	60.4	112	62.9	59.1	104	75.2	57.9
	98.9	96.3	71.8	59.1	115	64.3	56.7	106	73.5	57.9
	104	96.3	75.2	60.4	115	62.9	57.9	109	71.8	60.4
	102	93.8	70.2	60.4	115	65.7	56.7	112	77	59.1
	98.9	98.9	67.2	61.6	112	64.3	62.9	106	68.7	60.4
Mean	100.54	96.84	70.62	60.38	113.8	64.02	58.66	107.4	73.24	59.14
Stdev	2.354358	2.139626	3.079286	0.884308	1.643168	1.171324	2.570603	3.130495	3.191081	1.2502
Mpa value	985.9958	949.7099	692.5703	592.1467	1116.037	627.8441	575.2786	1053.272	718.2647	579.986

Table 10 Vickers Hardness compiled

5.9 SEM Images

SEM images were taken using BSE and SE mode on a Hitachi S-2600N SEM.

Incident electron beam interacts with the specimen as shown in the figure below. Change of Contrast to distinguish between 2 different phases is a typical characteristic of BSE. Secondary Electrons contain lower energy than the backscattered electrons and are very beneficial for the inspection of the topography of the sample's surface [20].

Hence both the modes were used in the study to easily understand the oxides present if any.

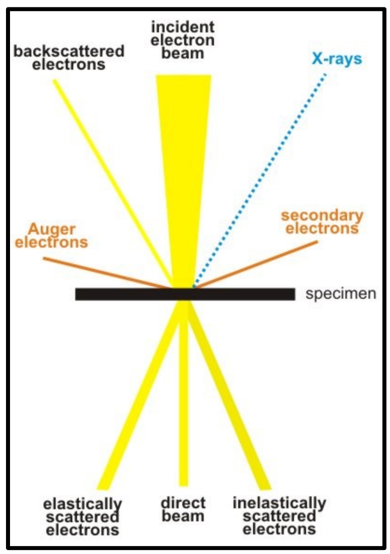

Figure 41 Interactions of Electrons with matter [21]

Polishing was done using 240,400,600,800&1200 grit silicon carbide papers. Final polishing was done using a vibratory polisher with 0.05µm alumina paste.

A mixture of Nitric Acid and distilled water (1:1 vol) was used to etch the grain boundaries.

5.9.1 Etched Coatings

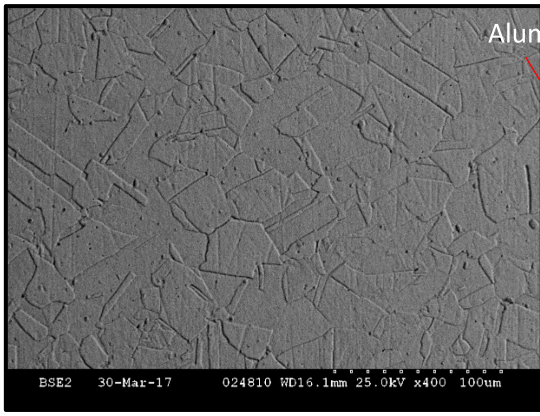

Figure 42 SEM Wrought Copper C-11000 BSE Mode

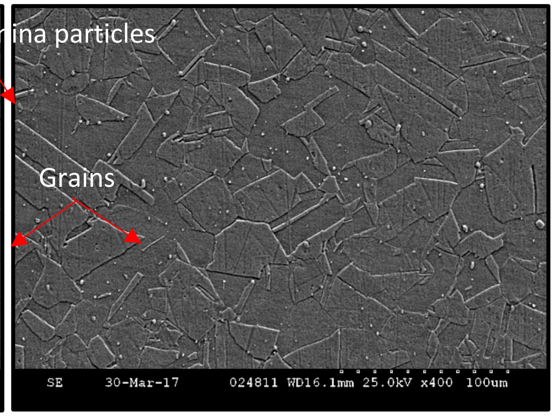

Figure 43 SEM Wrought Copper C-11000 SE Mode

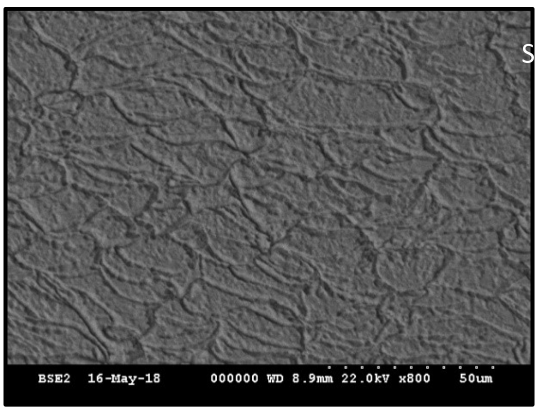

Figure 44 SEM As Sprayed Horizontal BSE mode

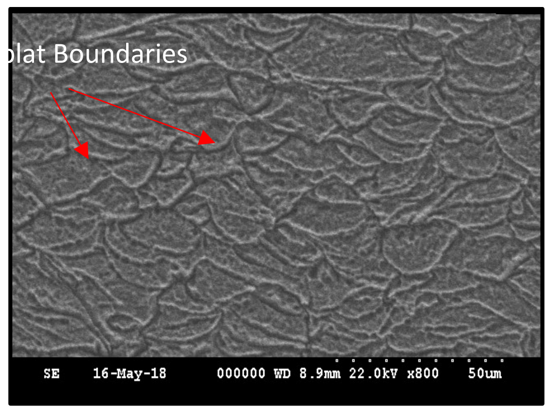

Figure 45 SEM As Sprayed Horizontal SE mode

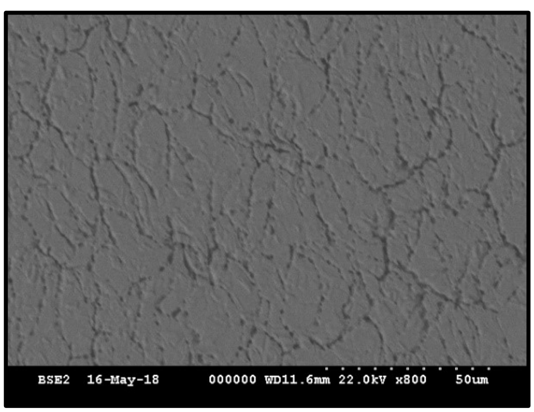

Figure 46 SEM As Sprayed Edge BSE Mode

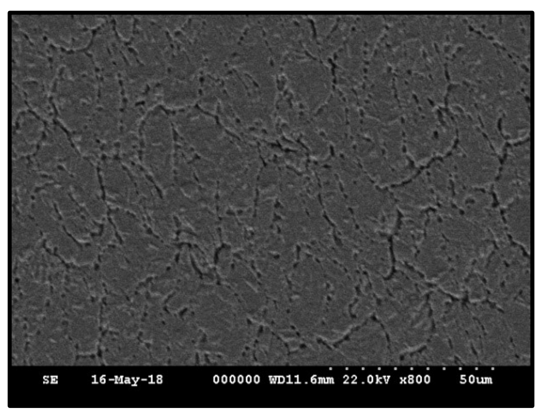

Figure 47 SEM As Sprayed Edge SE Mode

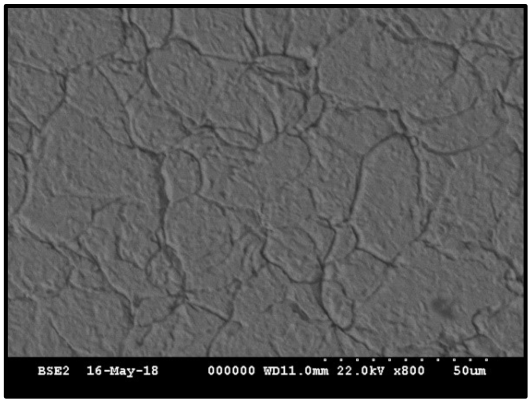

Figure 48 SEM As Sprayed Vertical BSE Mode

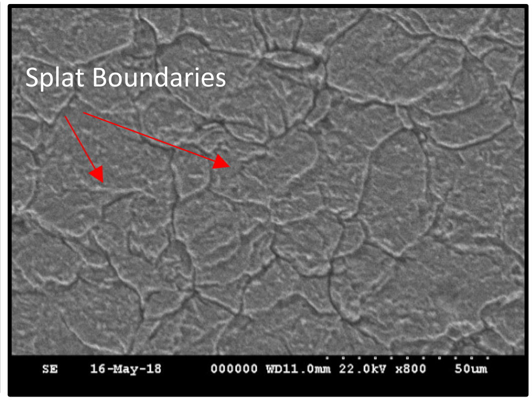

Figure 49 SEM As Sprayed vertical SE Mode

It clearly shows that microstructure varies according to the change in orientation of the sprayed coating. This thus aids to co-relate between the change in mechanical properties.

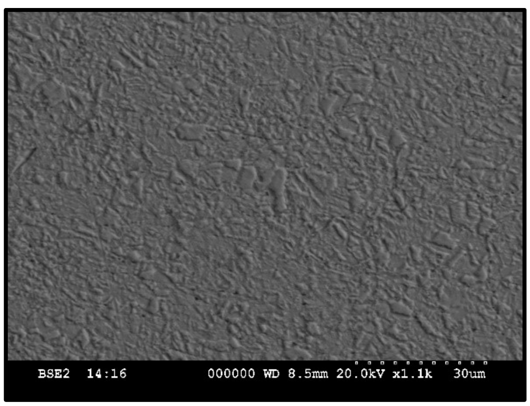

Figure 50 SEM 400C Heat treated Cu BSE Mode

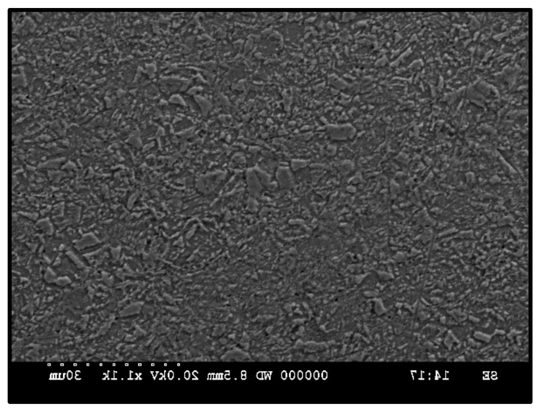

Figure 51 SEM 400C Heat Treated Cu SE Mode

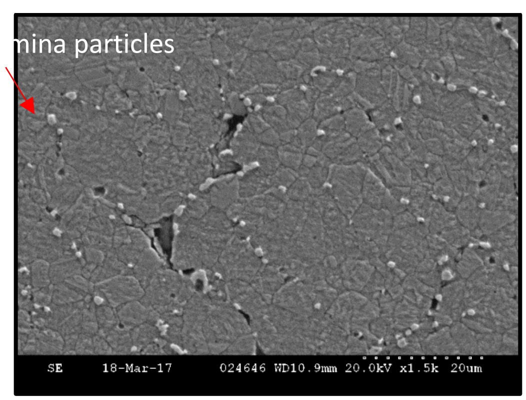

Figure 52 SEM 600C Heat Treated Cu BSE Mode

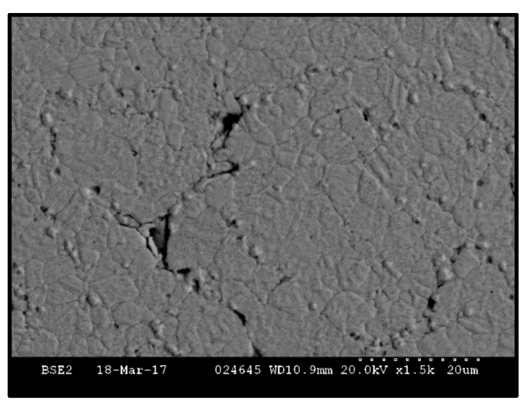

Figure 53 SEM 600C Heat Treated Cu SE Mode

Heat Treatment significantly affected the microstructure. Newly formed grains were visible at 400C annealing temperature. A uniform microstructure showing recrystallisation grains was visible for 600C heat treated samples [19].

5.9.2 Shear Punch Cracks

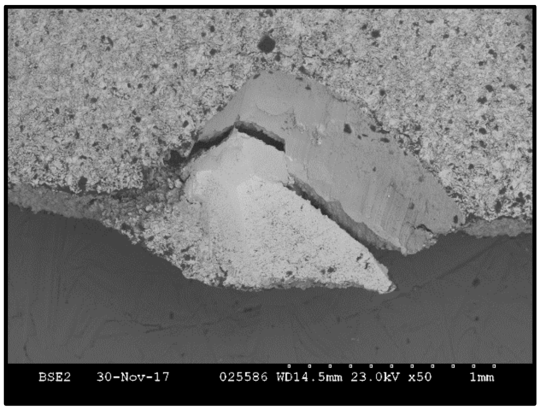

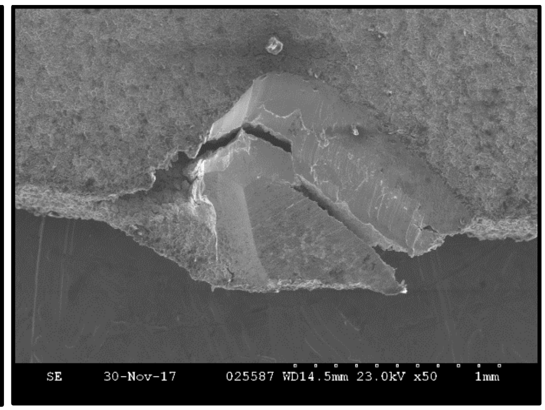

Figure 54 SEM SPT Crack As Sprayed Horizontal BSE Mode

Figure 55 SEM SPT Crack As Sprayed Horizontal mode

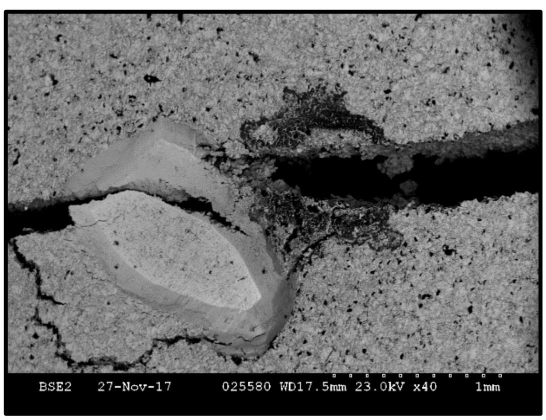

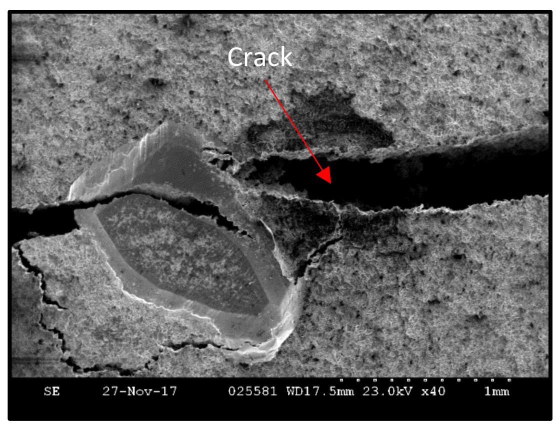

Figure 56 SEM SPT Crack As Sprayed Edge BSE Mode

Figure 57 SEM SPT Crack As Sprayed Edge SE mode

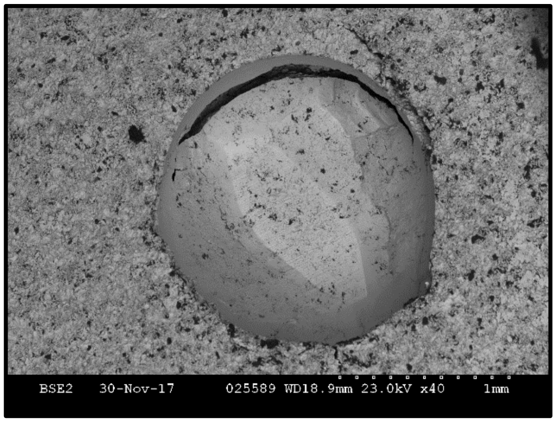

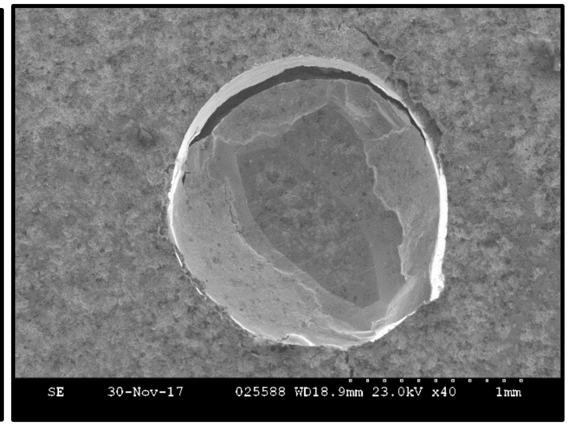

Figure 58 SEM SPT Crack As Sprayed Vertical BSE Mode

Figure 59 SEM SPT Crack As Sprayed Vertical SE Mode

Shear punch cracks were observed under the SEM. The SPT was carried out until the load on the UTM dropped from the peak.

Chapter 6
Conclusion and Future Study

6.1 Conclusion

An attempt for establishing a linear co-relation between shear strength and tensile strength of cold-sprayed copper was done in this study. This co-relation was validated for 3 different orientations of coatings. The effect of heat-treatment on the strength was also observed in terms of co-relation. Mechanical properties viz, hardness and electrical conductivity and the effect of heat treatment was also observed.

The as sprayed coatings displayed a linear co-relation of UTS (Ultimate tensile Strength) =1.9*USS (Ultimate Shear Strength) for 2 out of 3 sprayed orientations. This co-relation was close to that reported by Guduru et al [2] for wrought materials. It is suspected that the vertical orientation has a low mechanical strength relative to other orientations due to increase in the build-up layer. The heat-treated coatings displayed a linear co-relation of UTS=0.9*USS for all orientations.

The hardness properties didn't change with the orientation but significantly reduced/softened with heat treatment. The electrical conductivity also didn't change with the orientation; but improved with heat treatment. SEM images show with the increase in heat-treatment temperature a uniform recrystallisation is observed.

6.2 Future Study

A similar co-relation can be established for other cold-sprayed materials for eg: Aluminum, Steel and cross-referenced with wrought materials. Effect of laser on the mechanical properties of cold-sprayed materials can also be analyzed.

This miniaturized SPT can also be used for other thermal spray techniques viz, HVOF etc.

The SPT technique would thus aid the 3D printing industry to use this as a quality assurance tool. The technique would also save material making it cost-effective and quick.

References

[1] B. Kennedy and S. Calimari, "Spee3D," [Online]. Available: https://www.spee3d.com/.

[2] AMazing, "additive manufacturing.com," 2018. [Online]. Available: http://additivemanufacturing.com/basics/.

[3] M. R. Nichols, "Schooled by science," 2018. [Online]. Available: https://schooledbyscience.com/7-additive-manufacturing-categories/.

[4] V.K.Champagne, "Introduction," in *The cold spray materials deposition process- Fundamentals and applications*, Woodhead publishing, 2007, pp. 1-11.

[5] V. Varadarajan, "Development of a novel iron-manganese alloy and its application," University of Michigan-Dearborn, 2015.

[6] R. K. Guduru, K. A. Darling, R. Kishore, R. A. Scattergood, C. C. Koch and K. L. Murty, "Evaluation of mechanical properties using shear–punch testing," *Material Science and Engineering,* vol. 395, no. 1-2, pp. 307-314, 2005.

[7] G. L. Hankin, M. B. Toloczko, M. L. Hamilton, F. A. Garner and R. G. Faulkner, "Validation of the shear punch–tensile correlation technique using irradiated materials," *Journalof Nuclear Materials,* Vols. 258-263, no. 2, pp. 1651-1656, 1998.

[8] ASTM, "E8/E8M-16a Standard Test Methods for Tension Testing of Metallic Materials," *ASTM International,* 2016.

[9] H. Assadi, T. Schmidt, H. Richter, J. Kliemann, K. Binder , F. Gartner, T. Klassen and H. Kreye, "On Parameter Selection in Cold Spraying," *Journal of Thermal Spray Technology,* vol. 20, no. 6, pp. 1161-1176, 2011.

[10] S. Nagendiran, "METALLIZATION OF KEVLAR /SPALL LINER USING THERMAL SPRAY TECHNOLOGY," University of Michigan-Dearborn, 2016.

[11] C. Pasaquale , "Cold Spray Coatings," in *Recent trends and future perspectives* , Springer.

[12] W. Li, C. Zhang, X. Guo, G. Zhang , H. Liao, C. Li and C. Coddet, "Effect of standoff distance on coating deposition characteristics in cold spraying," *Materials and Design,* vol. 29, no. 2, pp. 297-304, 2008.

[13] I. S. University, "NDT Education," 2014. [Online]. Available: http://www.nde-ed.org/EducationResources/CommunityCollege/EddyCurrents/Applications/conductivitymeasurements.htm.

[14] C. D. A. Inc, 2018. [Online]. Available: https://alloys.copper.org/alloy/C11000.

[15] McMaster, 2018. [Online]. Available: http://www.mcmastercarr.com/.

[16] P. Precision, "Pivot Precision," [Online]. Available: https://www.pivotprecision.com/about-us.

[17] V. Karthik, "Tensile–shear correlations obtained from shear punch test technique using a modified experimental approach," *Journalof Nuclear Materials,* vol. 393, pp. 425-432, 2009.

[18] Iowa State University, Cowley County and Ridgewater, "NDT Resource Center," 1996. [Online].

[19] T. Stolenhoff, C. Borchers, F. Gartner and H. Kreye, "Microstructure and properties of Cold-sprayed and thermally sprayed copper coatings.," *Surface and Coatings Technology,* no. 200, pp. 4947-4960, 2004.

[20] S. Milne, "AZO Materials," 2018. [Online]. Available: https://www.azom.com/.

[21] F. Krumeish, "ETH Zurich," 2018. [Online]. Available: http://www.microscopy.ethz.ch/interactions.htm.